General Disclaimer

One or more of the Following Statements may affect this Document

- This document has been reproduced from the best copy furnished by the organizational source. It is being released in the interest of making available as much information as possible.

- This document may contain data, which exceeds the sheet parameters. It was furnished in this condition by the organizational source and is the best copy available.

- This document may contain tone-on-tone or color graphs, charts and/or pictures, which have been reproduced in black and white.

- This document is paginated as submitted by the original source.

- Portions of this document are not fully legible due to the historical nature of some of the material. However, it is the best reproduction available from the original submission.

E82-10350 SGT
CR-168969

STRUCTURE OF THE ST. FRANCOIS MOUNTAINS

AND SURROUNDING LEAD BELT, S.E. MISSOURI:

INFERENCES FROM THERMAL IR

AND OTHER DATA SETS

Quarterly Report 11/1/81 - 1/31/82

Quarterly Report 2/1/82 - 4/30/82

NAS5 - 26533

HCMM Data Analysis Program

R.E. Arvidson, P.I.
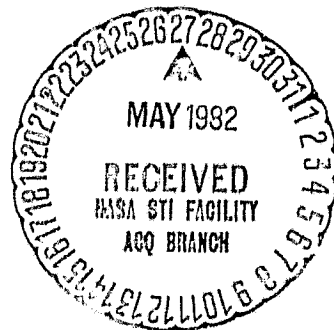
McDonnell Center for the Space Sciences

Department of Earth and Planetary Sciences

Washington University

St. Louis, Missouri 63130

May 11, 1982

RECEIVED

MAY 25, 1982

SIS/902.6

HFO-013

Type II

1. PROBLEMS: No problems were encountered during our analyses.

2. ACCOMPLISHMENTS:

1. Considerable effort was expended during the interval from
11/1/81 to 4/30/82 in revising the manuscript that we submitted to
the Journal of Geophysical Research in November, 1981. Although the
paper was accepted in its original form, we felt that revision was
needed. The manuscript dealt with the discovery of a Precambrian
rift running NW-SE through Missouri as seen in both free air and
Bouguer gravity anomalies and HCMM data. The revised manuscript is
attached. We have substantially changed the paper, including the
addition of magnetic field anomalies, basement rock types, and
seismic refraction profile data for the area. Of importance to this
study, we substantially revised the section on linears seen in
processed HCMM data covering the area. Included in the revised
paper is a discussion of what HCMM data were utilized and a map that
shows linear features seen from a merged daytime thermal image with
a shaded relief map of topography. Also drawn on the Figure (Figure
11 of the paper) are mapped faults and folds, and the outline of the
rift running through the state. HCMM linears were mapped separately
by three geologists, with the linears drawn on the figure being ones
seen by all three people. HCMM linears in some cases correspond to
mapped features, in some cases they are extensions of mapped
features, and in some cases they do not correspond to any mapped
structure. The linears correlate nicely with the trend of the
Precambrian rift as seen in the gravity data, suggesting that the

linears are indeed related to the underlying basement structure.
The pattern of faulting is consistent with uplift, suggesting that
the rift is isostatically readjusting. HCMM data proved to be
particularly useful because the synoptic coverage and the broad
pixel width in effect filtered out all but regional-scale
structures.

The reason that JGR paper took so long to revise and the reason
that these quarterly reports are delayed is that we were invited by
the editor of EOS (Transactions, American Geophysical Union) to
submit a paper on our Missouri rift, stressing digital image
processing of potential field and topographic data. That paper is
also attached - it appeared in the May 4, 1982 issue of EOS, with
our color gravity maps on the cover.

2. Attached are HCMM daytime thermal IR, night time thermal
IR, and apparent thermal inertia images that have been
contrast-enhanced and transformed to Mercator projections. Also
attached is a daytime IR overlain onto a shaded relief map and an
apparent thermal inertia image overlain onto a shaded relief map.
Frame numbers are A-A0045-19420-2, A-A0045-19420-1, and
A-A0044-08310-3. These products were processed and used as part of
a Masters Thesis finished in May 1, 1982 by John Strebeck. In the
thesis Strebeck examined correlations between the HCMM data
products, linears, and geologic units. The significant results are
included in the attached J.G.R. paper. The thesis reference would
be:

Strebeck, J.W., 1982, Structure of the Precambrian basement in the
Ozark Plateau as inferred from gravity and remote sensing data,

Master of Arts Thesis, Washington Univ., 149 p., available
Univ. Microfilms, Ann Arbor, Michigan.

Strebeck now works with Mobil Oil Corp., Dallas, Texas, where he
should be joining their remote sensing/image processing group after
preliminary "indoctrination" into the company.

3. We have begun to examine the difference in information
content between day IR, night IR, albedo, and thermal inertia
images. For the frames listed above, the day IR image was found to
have the greatest discriminability for rock types and with regard to
structural patterns. The reason seems to be primarily due to
topography in that most geologic units in southern Missouri exhibit
a distinctive topography and most structural features that we have
mapped are controlled by the distribution of stream valleys. The
day IR image best expresses these distributions because the
brightness (relative temperature) is sensitive to differential solar
heating due to slopes. For the three frames discussed above, the
day IR contained 0.63 of the fractional variance of the three data
sets, while the night IR contained 0.12 and the albedo data
contained 0.25. Apparent thermal inertia images should provide an
indication both of topographic roughness (since slope effects on
differential solar heating have not been removed) and an indication
of thermal anomalies that are controlled by variations in soil or
rock exposure, vegetation type, and moisture content. We are
presently concentrating on delineation of these latter features,
i.e., identifying linears in southern Missouri that are not directly
controlled by topography.

4. We have also coded the thermal IR and albedo data as hue, saturation, and brightness values to generate a color display, following the work of Haydn, University of Munich. However, we find that the transformation used by Haydn to go from hue, saturation, and brightness to red, green, and blue images is only correct for relatively narrow hue range. A universal derivation is attached, along with a color print where the day, night, and albedo images have been encoded as hue, brightness; and saturation. A color print is also included that has the apparent thermal inertia coded in a color spectrum and overlain onto a shaded relief map.

3. FUTURE WORK:

1. Presentation of results of analyses of HCMM data as part of a paper to be presented at COSPAR, Ottawa, Canada, on May 19, 1982, entitled:

Arvidson, R.E., E.A. Guinness, J.W. Strebeck, 1982, Structure of the Midcontinent basement - Topography, gravity, seismic, and remote sensing data.

and included in the session on Geophysical Measurements of Major Crustal Features From Space.

2. An oral presentation of our HCMM work at the spring meeting of the American Geophysical Union, Wash., DC. during the week of May 31, 1982. The abstract is attached and entitled:

Strebeck, J.W., E.A. Guinness, R.E. Arvidson, 1982, Linear Structures in Missouri seen with Heat Capacity Mapping Mission

Given 3 images and treating each as a separate component of color it is possible to create a color image which contains information from all three original datasets. One possible application is to take HCMM albedo, day IR, and night IR and treat them as brightness (r), hue (α), and saturation (γ) respectively. Each point (r, α, γ) can be mapped into a point in "normal" color space; that is, a red, blue, and green intensity level.
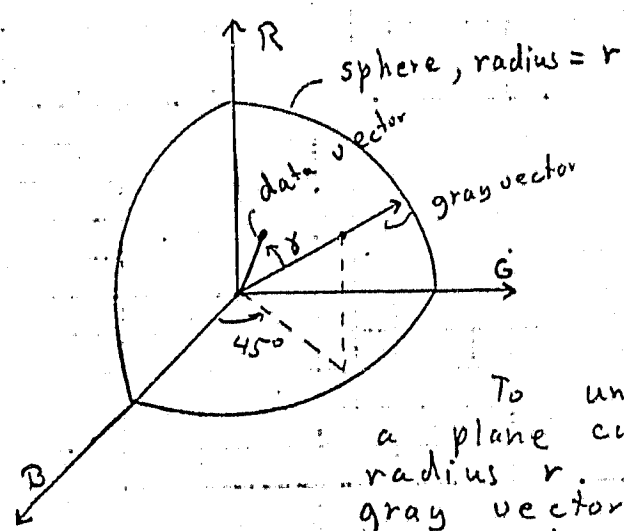
Method:

Solve for f in:

$$\begin{pmatrix} r \\ \alpha \\ \gamma \end{pmatrix} = f \begin{pmatrix} B \\ G \\ R \end{pmatrix}$$
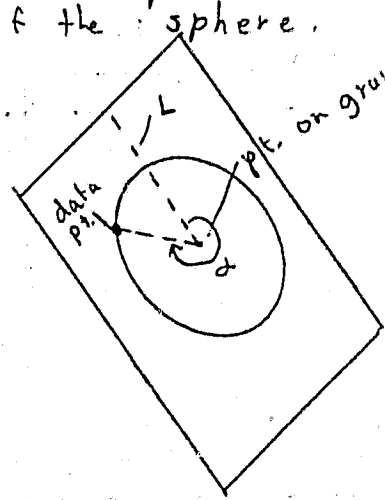
B = blue intensity
G = green "
R = red "

Geometry:

A data vector is defined by (r, α, γ) where

r = magnitude (length) of the vector

γ = angle between the gray vector and data vector

To understand α, we look at a plane cutting through the sphere of radius r. The plane is $\perp$ to the gray vector and contains the data point plus a circular cross-section of the sphere.

α is defined by a line drawn in our plane which intersects both the gray vector point shown, and the point defined by the intersection of the plane and the R-axis. This is the line L. Then α is the negative angle (in the sense of the right-hand-rule using the gray vector) between L and the line connecting the data point and the gray vector.

Set up a coordinate system O with axes x, y, and z such that the y-axis lies in the B-G plane and the x-axis lies along the gray vector.
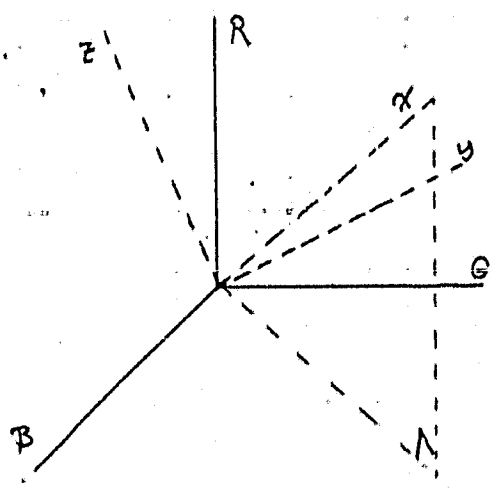
Then in O, we have

— sphere's projection onto x-z plane
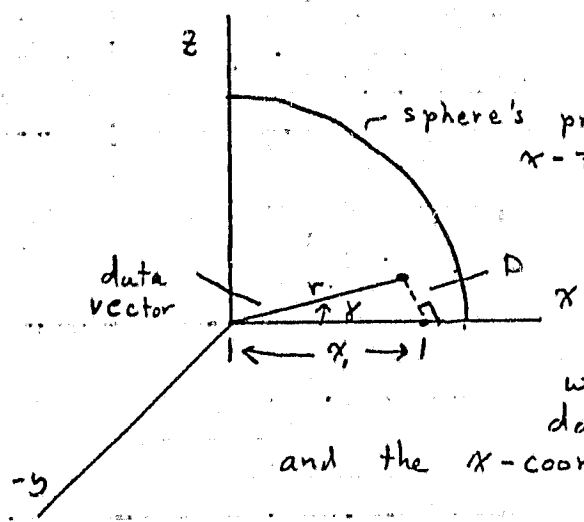
$$D = r \sin \gamma$$

where D is the $\perp$ distance from data point to x-axis (gray vector)

and the x-coordinate of the data point is

$$x_1 = r \cos \gamma$$

Now, to find y_1 and z_1, use α

$y_1 = D \sin \alpha$

$z_1 = D \cos \alpha$

so from $\begin{pmatrix} r \\ \alpha \\ \gamma \end{pmatrix} \Rightarrow \begin{pmatrix} x_1 \\ y_1 \\ z_1 \end{pmatrix}$

To get B, G, R from x, y, z we simply rotate coordinate axes into alignment.

YROT is the angle through which the 0 coord. system must be rotated about the y-axis to put the x-axis into the B-G plane and the z-axis into alignment w the R-axis

$YROT = \tan^{-1}\left(\frac{1}{\sqrt{2}}\right)$

$\cong 35.26°$

It is then a simple matter to rotate thru $-45°$ about the z-axis and align the x and y axes to the B and G axes respectively.

Boundary condition: Normalizing γ

Since the input values of γ range from 0 to 255 and the allowed angles γ range from $0°$ to $\tan^{-1}(\sqrt{2})$ ($\sim 55°$), we must fit γ into that range.

There is an additional problem. Taking $\gamma = \gamma_{max}$ and using all possible values of α ($0° \rightarrow 360°$), a cone is swept out. The cone is shown below in relation to the R-G, G-B, and B-R planes. The plane of the paper is the same plane used before to illustrate α; it is normal to the gray vector.
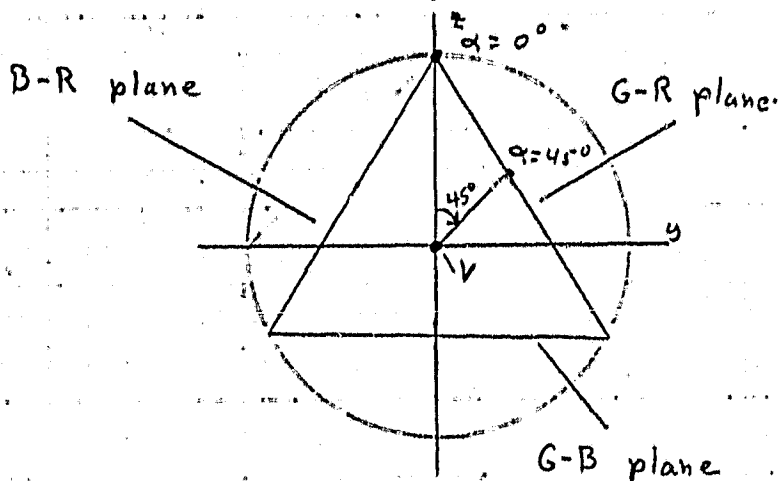
The point V is the intersection of our plane and the gray vector. Taking $V = (255, 0, 0)$ ($x = 255, y = 0, z = 0$), it is quite obvious that $\gamma_{max}(\alpha = 0°) \neq \gamma_{max}(\alpha = 45°)$

That is, if $\gamma_{max} = 55°$ were used for all α's, then data points would be created that would fall to the outside of the triangle created by the RGB coordinate system. In effect, the results would be negative color intensities.

We are helped along by several facts

1) γ_{max}, the angular distance between the gray vector and any color axis (R, G, or B) is given by $\tan^{-1}(\sqrt{2})$

2) γ_{min}, the angle between the gray vector and any color plane along the normal to that plane is given by $\tan^{-1}(\frac{1}{\sqrt{2}})$

3) V is at a distance of 255 DN from the origin of both the color coordinates and O.

To find γ', the normalizing factor, we must then find a distance DIST where

DIST is a function of α such that
$$\text{DIST}(0°) = \text{DIST}(120°) = \text{DIST}(240°)$$
$$\text{DIST}(60°) = \text{DIST}(180°) = \text{DIST}(300°)$$
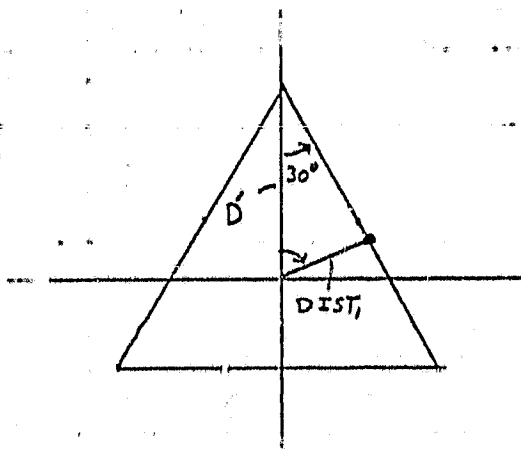
and

$$\gamma' = \tan^{-1}\left(\frac{\text{DIST}}{255}\right)$$

γ' varies from $\tan^{-1}(\sqrt{2})$ to $\tan^{-1}(1/\sqrt{2})$

There are three cases for $\gamma'(\alpha)$

Case I) $0° \leq \alpha \leq 120°$

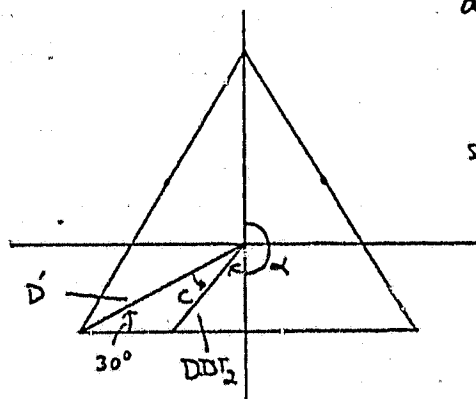By the Law of Sines
$$\frac{\sin 30°}{\text{DIST}_1} = \frac{\sin(180° - 30° - \alpha)}{D'}$$

$$\text{DIST}_1 = \frac{.5 D'}{\sin(150° - \alpha)}$$

Case II) $120° \leq \alpha \leq 240°$

$c = (270° - 30°) - \alpha = 240° - \alpha$

and
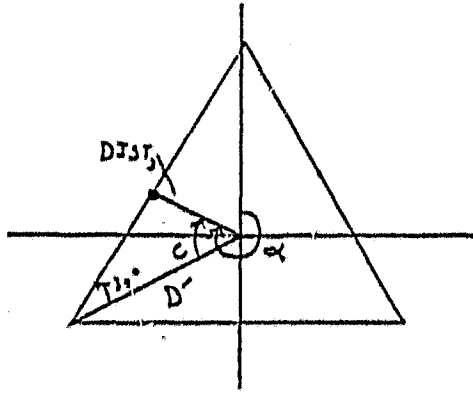
$$\frac{\sin 30°}{\text{DIST}_2} = \frac{\sin(150° - c)}{D'}$$

so
$$\text{DIST}_2 = \frac{.5 D}{\sin(90° - \alpha)}$$

$$= -\frac{.5 D}{\cos \alpha}$$

Case III) $\alpha > 240°$

$$c = \alpha - (60° + 180°)$$

$$\frac{\sin 30°}{DIST_3} = \frac{\sin(150° - c)}{D'}$$

so

$$DIST_3 = \frac{.5\,D'}{\sin(150° - c)}$$

$$= \frac{.5\,D'}{\sin(30° - \alpha)}$$

Taking γ_0 to be the input value for γ

$$\gamma' = \tan^{-1}\left(DIST_n / 255\right)$$

and

$$\gamma = \gamma_0 \cdot DN \times \left(\frac{\gamma'}{255\,DN}\right)$$

Next we find D'
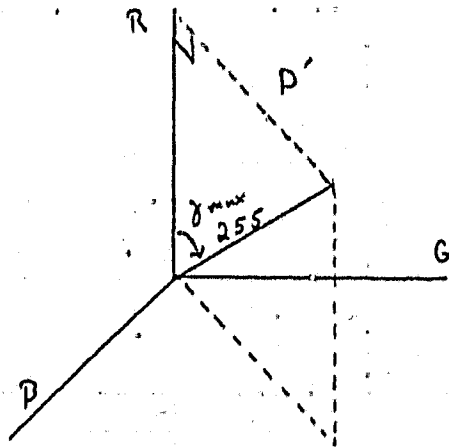
From the figure to the left,
since $\gamma_{max} = \tan^{-1}(\sqrt{2})$

and $\gamma_{max} = \tan^{-1}\left(D'/255\right)$

$$D' = \sqrt{2}\,(255)$$

so finally we can take

$$\gamma = \frac{\gamma_0}{255} \times \tan^{-1}\left(\frac{D_n}{\sqrt{2}}\right) \qquad n = 1, 2, 3$$

$$D_n = \begin{cases} \frac{1}{\sin(150° - \alpha)} & 0° \le \alpha \le 120° \quad n=1 \\ -\frac{1}{\cos\alpha} & 120° < \alpha < 240° \quad n=2 \\ \frac{1}{\sin(30° - \alpha)} & 240° \le \alpha \le 360° \quad n=3 \end{cases}$$

IDENTIFICATION OF A PRECAMBRIAN RIFT THROUGH

MISSOURI BY DIGITAL IMAGE PROCESSING

OF GEOPHYSICAL AND GEOLOGICAL DATA

E.A. Guinness, R.E. Arvidson, J.W. Strebeck,

K.J. Schulz, G.F. Davies and C.E. Leff

Department of Earth and Planetary Sciences

McDonnell Center for the Space Sciences

Washington University

St. Louis, Missouri   63130

ABSTRACT

Digital free air and Bouguer gravity anomaly images have been constructed for the region bordered by 25° to 49° N. lat. and 80° to 110° W. long. from approximately 287,000 station readings. The technique used to interpolate between station locations was based on a two dimensional spatial filter, where the average of the anomaly values located within the filter area was computed. The images contain as many as 256 contours (values in byte variable), so that subtle anomaly patterns can be identified and traced with much greater certainty than on most contour maps. A newly discovered feature in the midcontinent is a gravity low that begins at a break in the midcontinent gravity high in S.E. Nebraska, extends across Missouri in a NW-SE direction, and intersects the Mississippi Valley graben to form the Pascola arch. The anomaly varies from 120 to 160 km in width, extends about 700 km, and has a medial gravity high for part of its length. The maximum Bouguer amplitude of the anomaly is approximately 34 milligals below values for the surrounding region and cannot be explained on the basis of a thickened section of Paleozoic sedimentary rock. The gravity data and the sparse seismic refraction data for the region are consistent with an increased crustal thickness beneath the gravity low. Discrete positive magnetic anomalies, some of which correspond to mafic intrusives, are concentrated along the borders of the gravity low. Digitally enhanced thermal infrared images from the Heat Capacity Mapping Mission show a distinct alignment of linear structures with the gravity feature. The linears in some cases correspond to mapped

high angle normal faults, to drape folds over relief within the Precambrian basement, and in some cases to extensions of mapped structures. The gravity anomaly also cuts across the major Precambrian boundary in S.E. Missouri marking the change from older, sheared granites and metasedimentary rocks, to younger granites and rhyolites. Given the cumulative evidence, the gravity anomaly is probably the present expression of a failed arm of a rifting event, perhaps one associated with the spread'ng that led to or preceeded formation of the granite and rhyolite terrain of southern Missouri.

INTRODUCTION

We have been pursuing relationships between the pattern, age, and origin of structural features within the Precambrian basement rocks of southern Missouri and the locations and genesis of ore deposits. The area is a well known lead mining district, where Mississippi Valley type Pb-Zn-Cu ores have accumulated in Cambrian carbonate rocks associated with stromatolitic reef and backreef facies (Gerdemann and Meyers, 1972). The location of these facies was controlled by the location of the shore line, which was in turn controlled by the pattern of faulting of the Precambrian basement (Grundmann, 1977; Sweeny et al., 1977; Evans, 1977; Paarlberg and Evans, 1977; Mouat and Clendenin, 1977). In addition, iron ores of magmatic origin can be found in the Precambrian basement rocks along fracture zones (Kisvarsanyi , 1976).

Structural studies of basement rocks in southern Missouri have been pursued for a considerable amount of time (see: Kisvarsanyi

and Kisvarsanyi, 1976), and a significant amount of information has been gained on the distribution of Precambrian rock types and ages (Kisvarsanyi, 1974; Bickford et al., 1981; VanSchmus and Bickford, 1981). However, little has been done in terms of understanding how the structure of the region is related to the overall structural configuration of the midcontinent or how such features are related to the structural history of the area. In this paper we utilize digital image processing techniques to reduce and display a variety of potential field, topography, geologic, and remote sensing data for the midcontinent. The intent is to delineate how structural patterns in southern Missouri are related to the broader features of the midcontinent.

DISCRIPTION OF DATA AND PROCESSING METHODS

Digital image processing techniques have a potentially wide range of utility for display and analysis of geographically (i.e., array) oriented data sets. In our case, data covering the midcontinent were processed on a PDP-11/34 minicomputer with interactive image display peripherals, using standard digital image enhancement, filtering, and geometric operations. The reader is referred to standard texts such as Moik (1980) for further information on image processing techniques, and to Arvidson et al. (1982) for examples of the utility of image processing in processing, display, and interpretation of topographic and gravity data for the continental United States.

National Oceanic and Atmospheric Administration (NOAA) digital

topography, together with land station measurements of gravitational acceleration, comprise two important data sets that we employed in the study. The area chosen for analysis of the topography and gravity ranges from 25° to 49° N. lat. and 80° to 110° W. long., thereby covering regions from the eastern edge of the Rockies on the west to the Appalachians on the east, and from the Superior Province on the north, to the Gulf of Mexico on the south. The topography consists of average elevations for areas covering 30 seconds in both latitude and in longitude. Gravity stations are typically spaced three km apart, but vary between hundreds of meters to ten kilometers over the study area. The gravity data were reduced to free air and to Bouguer anomalies courtesy of the Defense Mapping Aerospace Agency Center, St. Louis, Missouri. The reference field at sea level used was based on the 1967 International Gravity Formula, with all the data referenced to the 1971 International Gravity Standardization Net. Bouguer anomalies were computed based on a slab model with a density of 2.67 gm/cm3. No local terrain corrections were included.

Magnetic anomalies were also included in the analysis. Unfortunately, digital data for the region were not available at a reasonable cost. Consequently we restricted inclusion of magnetic coverage to the state of Missouri, based on the 1943 statewide contour map of vertical field intensity anomalies. The state map was photographed onto film and then the film was digitized, resulting in a digital image of magnetic anomaly contours for Missouri. Similarly, the basement rock type map for the midcontinent compiled by Bickford et al. (1981) and VanSchmus and

Bickford (1981) was transformed to a digital format for use in comparison with other data sets.

Other digital data sets that were utilized in this work included Heat Capacity Mapping Mission (HCMM) images. HCMM consisted of a satellite with sensors capable of imaging the surface in the visible to the reflected infrared (0.5 to 1.1 micrometers) and in the thermal infrared (10.5 to 12.5 micrometers) (Price, 1977). Each image element in the HCMM data covers about 500m across and one scene covers about 700 km in width and in height. The visible-reflected infrared sensor was used to measure the broad band albedo of the surface, while thermal infrared data acquired during the day and night provided information on the magnitude of diurnal temperature changes. These parameters can be used to solve for the thermal inertia of the surface, a thermophysical property that depends on the density, thermal conductivity, and specific heat (Kahle et al., 1976). Thermal infrared data, including estimates of thermal inertia, have been shown to be useful in delineating structural features in a variety of geological contexts (Sabins, 1969; Offield et al., 1975; Watson, 1981). HCMM data were included in this study both because of the applicability of thermal data in structural studies and because the synoptic view is appropriate for examining the surface expression of regional-scale structures. HCMM images for southern Missouri were contrast enhanced, digitally registered to one another, and displayed in a variety of formats designed to emphasize structural trends. Details of HCMM processing techniques will be discussed in a later section.

The first step in the analysis of topographic and gravity data

was to scale the dynamic range of the data to fit within the range of a byte variable (i.e., 8 bits or 256 discrete values). The byte data were then stored in image arrays, registered to a common base if needed, and processed. Final displays were transformed to Mercator projections and overlayed with latitude-longitude grids. The byte-encoded topographic data were first stored in an array with 30 second spacing in both latitude and longitude. The data could be displayed as an image if the byte-encoded values were converted to brightness or to color values. Alternatively, a shaded relief image could be constructed if a photometric function for the surface is assumed. Figure 1 shows a shaded relief image transformed to a Mercator projection and depicting topography under the assumption that the surface obeys Lommel-Seeliger scattering law (Batson et al., 1975). The simulated sum is from the northeast at 20° above the horizon.

Generation of images from the gravity anomaly values is more complicated than generating displays from the topographic data. The reason is that the gravity stations are not located along regular grid intersections. We chose a simple, but powerful spatial filtering technique for interpolating between station locations. The byte-encoded anomaly values were first assigned to array locations closest to the station locations. This procedure produced an array in part occupied by valid data and in part occupied by blank zones. The filtering algorithm that we then applied was developed by Eliason and Soderblom (1977), used to produce topographic maps from the Pioneer-Venus altimetry data (Pettengill et al., 1980), and applied to generating gravity images for the

continental United States by Arvidson et al. (1982). The technique involves use of a spatial filter of N x N elements. The average of the valid data points within any given filter location is computed and used to replace the midpoint value, but only if a valid datum does not already exist at that array location. In practice, the gravity data were processed using several filter passes, beginning with a 3 x 3 element filter and ending with a 21 x 21 element filter. The choice of filter sizes'was governed by station spacings, which varied from hundreds of meters to ten kilometers. The result is an interpolated data set, except for regions that had so few valid data points that a user-defined threshold was not met. In our case, we set the threshold so that at least 20% of the elements for any filter position would have to have been occupied by valid data for an interpolation calculation to proceed.

The interpolated gravity data can be displayed as a gray tone image, as is done in Figure 2 for free air anomalies. Black areas in the image correspond to zones with too few stations to allow valid interpolations. The gravity data can also be displayed as a shaded relief image, where gravity highs and lows are illuminated as if they were hills and valleys. Figure 3 is a shaded relief image of the free air anomalies with the simulated sun placed at 15° above the northeastern horizon.

The gravity anomaly images displayed in Figures 2 and 3 and equivalent Bouguer anomaly presentations have been checked against published maps (e.g. Woolard and Joesting, 1964; McGinnis et al., 1979; Simpson and Goodson, 1981). Generally the images and published maps correspond. However, the images have intrinsically

more information displayed, for at least three reasons. First, the grid spacing used to interpolate between station readings is more closely spaced than the spacing used to generate most published continental-wide contour maps. Second, there can be as many contour intervals in our displays are there are values in a byte (256). Third, because of the particular filtering algorithm used, areas with closely spaced stations retain local details of anomaly patterns. For instance, Figures 2 and 3 show a major gravity feature (free air low) that begins at a break in the midcontinent gravity high and extends about 700 km to the southeast. One of the distinguishing aspects of this feature is not the amplitude of the low but rather the sharp gravity gradient associated with the edges of the anomaly. Although sections of the feature have been noted in the past (see: Phelan, 1969; Cordell, 1979; Russ, 1981), the images shown in Figures 2 and 3 provide new information and a broader perspective that show the trend and location much more accurately than can be seen in published maps.

Finally, an important aspect of comparing data sets is the ability to merge or overlay one data set onto another to produce a visual display that maximizes the eye's ability to see correlations between the data sets. A useful technique is to allow one data set (gravity anomalies, for instance) to control the hue (dominant wavelength) and saturation (degree of purity) of a color image, while another data set (topography, for instance) controls the color brightness (Arvidson et al., 1982). Also, it is possible to combine values of a given parameter with a shaded relief presentation of that parameter by allowing the value to control the color hue and

saturation, while the local gradient, expressed in shaded relief form, controls the brightness (Pettengill et al., 1980; Kobrik, 1982). For example, Figure 4 is a version of the free air image where the anomaly values have been color-coded and overlain onto a shaded relief version of the anomalies. The effect is to produce an enhancement showing information related both to the value of the anomaly and to the local gravity gradient.

BASEMENT STRUCTURE IN MISSOURI AS DEFINED
BY GRAVITY ANOMALIES AND SEISMIC PROFILES

Figure 5 is a sketch map showing the major structural features seen in the free air anomaly images shown in Figures 2, 3, and 4 and in Bouguer images covering the same region. The free air data facilitated mapping of major topographic features associated with the Cordillera, Ouachitas, and the Appalachians. The Bouguer data provided new information that allowed us, for instance, to map the strong positive anomalies associated with the Mississippi embayment.

The midcontinent gravity high is a major gravity anomaly in the midcontinent. In our data this feature has a maximum free air anomaly of 85 milligals and a maximum Bouguer anomaly of 50 milligals. The midcontinent gravity high is about 70 km wide, contains Keewanawan basalts that date at 1.1 Ga, and has been interpreted as a failed continental rift (Chase and Gilmer, 1973). Flanking lows on either side of the high have been modeled as thick (several kilometers) arkosic sediments deposited as the load associated with the basalts caused regional subsidence.

Considerable structure an also be seen in the greenstone-granitic terrain of the Superior Province located to the northwest of the midcontinent gravity high. The Wisconsin Arch, the Ouachitas, and the Wichita-Arbuckle system are just a few of the other features that have a recognizable gravity signatures. For reference, the Quachitas have a maximum free air and Bouguer anomaly magnitudes of 76 and 54 milligals below the surrounding regions.

A subtle, but pervasive gravity feature seen in both the free air and Bouguer images is a linear low that begins at a break near the southeastern end of the midcontinent gravity high (40.5° N. lat., 96° W. long.), strikes in a southeasterly direction, and extends to the Mississippi Embayment (36° N. lat., 90° W. long.). The low varies between 120 to about 160 km in width, extends about 700 km in length, and for part of its length exhibits a medial gravity high. The maximum Bouguer anomaly associated with the low is about 34 milligals below values for surrounding regions. The feature begins just to the northwest of Missouri and ends just beyond the southeastern boundary of the state. We therefore informally refer to the feature as the Missouri gravity low. As discussed in Arvidson et al. (1982), the intersection of the Missouri gravity low with the Mississippi Valley graben as defined by Kane et al. (1981), is the site of the majority of the microseismic epicenters recorded in the 1970's by the St. Louis University seismic network (Stauder et al., 1977). In addition, the northern boundary of the intersection is the site of the circular Bloomfield anomaly, while the southern boundary is the site of the Covington anomaly. Both features can be seen in the free air and

Bouguer data as distinct, circular positive anomalies. Kane et al. (1981) suggest that these two anomalies, which are also positive magnetic anomalies, are due to intrusions of magmas during the Mesozoic Era. The intersection of the Missouri gravity low and the Mississippi Valley graben is also the site of the Pascola arch as defined by Phelan (1969) and Ervin and McGinnis (1975).

Several gravity profiles were generated across the Missouri gravity low to illustrate its form and to model subsurface density configurations. The location of the southern-most profile is shown in the sketch map in Figure 5. Values for the topography, free air, and Bouguer anomalies for this profile are shown in Figure 6. A simple model for the anomaly would be a thickened section of relatively low density sedimentary rock overlying a downwarped region of the Precambrian basement. However, drill holes covering the general area of the profile A-A' indicate a typical cover of Paleozoic sediments of only a few hundred meters over the low, with no discernable thinning on either side (Kisvarsanyi, 1974). Thus, the gravity signature must be related to a inhomogeneity within the Precambrian basement rocks. Cordell (1979) reached a similar conclusion for that part of the low located in the southwestern part of the Rolla quadrangle (37° to 38° N. lat.; 90° to 92° W. long.), where there is a slight local thickening of sedimentary cover over the gravity low.

Some seismic data exist for Missouri that provide information on the possible subsurface configurations of the crust that would give rise to the observed gravity anomaly patterns. Stewart (1968) conducted a reversed seismic refraction survey of about 300 km in

length along an east-west line in northern Missouri crossing the gravity low at about 39.8° N. lat. Results indicate that the crust consists of three major layers, with average depths of about 5, 20, and 40 km and a 3/4 degree of dip toward the west. Stewart (1968) also conducted a reversed profile in southern Missouri that extends across the gravity low at about 50 km to the northwest of the gravity profile A-A' (Figure 5). The refraction data for Stewart's (1968) southern profile exhibit very low signal/noise ratios, perhaps because of significant lateral inhomogeneities within the crust. Results are compromised by the low quality of the data, although an arguement can be made for a thickened crustal section in the southwestern half of the profile and somewhat higher crustal velocities beneath the northeastern half of the traverse (Nuttli, 1976). Finally, McCamy and Meyer (1966) conducted a seismic refraction survey from Little Rock, Arkansas to Cape Girardeau, Missouri, reversing a survey done several years earlier. The refraction profile cut across the Bloomfield gravity anomaly and ran in a NE-SW direction within the Mississippi embayment (i.e., to the southeast of profile A-A' of Figure 5). As discussed by Ervin and McGinnis (1975), this region is unusual in that the crust is slightly thicker and underlain by an anomalously high velocity layer as compared to Stewart's (1968) profile in northern Missouri. The anomalous layer probably corresponds to high density material at the base of the crust, material that may have been emplaced in association with the Precambrian rifting that produced the Reelfoot rift.

In summary, the seismic data suggest a slightly thicker crustal

section under the Missouri gravity low, although this interpretation
is compromised by poor data and the complicating influence of rocks
associated with processes that probably lead to formation of the
Mississippi embayment. If it is assumed that the Missouri gravity
low is due to a thickened crust, then a 34 milligal anomaly, and a
density contrast of 0.3 gm/cm3 between crust and mantle, is
consistent with a crustal excess of about 3.3 km under the anomaly
(Strebeck, 1982). Alternatively, if it is assumed that lateral
density variations cause the gravity anomaly, than the anomaly would
be consistent with rocks that were 0.1 gm/cm3 less dense than
surrounding materials for the first 4 to 8 km below the surface
(Strebeck, 1982). Of course, other models of crustal
inhomogeneities can be generated. However, in the absence of other
constraints, they are not worth pursuing at this point.

RELATIONSHIP OF MISSOURI GRAVITY LOW TO
PRECAMBRIAN ROCK PROVINCES AND TO
MAGNETIC ANOMALIES

Information on the distribution of Precambrian rock types in
Missouri is limited because of the relatively few drill holes that
have penetrated into the basement and because of the complexity of
the Precambrian geology in the area (Kisvarsanyi, 1974; Bickford et
al., 1981; VanSchmus and Bickford, 1981). There is, however, a
major boundary between 1.6 Ga old rocks composed largely of sheared
granites and metasediments, and younger 1.4 Ga old granites and
rhyolites. The boundary runs in a NE-SW direction, as is shown in

Figure 7, where the basement rock map of Bickford et al. (1981) has been overlain onto a shaded relief map depicting Bouguer anomalies. The Missouri gravity low cuts across the boundary at nearly right angles. There is also clearly an extension of what are thought to be older metasedimentary rocks into the younger terrain along the gravity low. Kisvarsanyi (1974) notes that the area containing the reentrant of older rocks is also a structural high on contour maps depicting the paleotopography of the Precambrian surface and on structured contour maps of Paleozoic sedimentary formations. Presumably, older Precambrian rocks are exposed along the low because of isostatic readjustment and erosion of the younger granites and rhyolites preferentially along the feature.

The observation that the gravity low cuts across the major Precambrian age and rock type boundary in Missouri suggests that the low is related to a structural feature. Further support for this suggestion can be found in the locations of areas with discrete, positive magnetic anomalies. Figure 8 shows regions with vertical intensity magnetic anomalies higher than 600 gammas as black splotches superimposed on the gray tone and shaded relief versions of Bouguer anomalies for Missouri. The 600 gamma contour interval was chosen on the basis of delineating discrete magnetic highs. The magnetic highs are in part clustered along the flanks of the gravity low, i.e., where the gravity gradient is high. Other magnetic highs coincide with discrete gravity highs, such as in the area underlain by the Bloomfield intrusion in southeastern Missouri or the Salem intrusion in the middle of the gravity low (Figure 8). Clearly, more work needs to be done to establish the pattern of magnetic

anomalies in more detail, along with establishing the relationship
of the anomaly patterns and the gravity low. Examination of
unpublished maps constructed by I. Zietz supports the observation
that the magnetic highs are along the flanks of the gravity low.

Previous work shows that some magnetic highs in Missouri can be
correlated with relatively iron rich igneous rock bodies (Phelan,
1969; Cordell, 1979). The location of the discrete magnetic highs
long the flanks of the gravity low suggests that the flanks
correspond to zones of weakness where magmas have been intruded.
Kane et al. (1981) note a similar correlation of magnetic highs
along the perimeter of the Mississippi Valley graben. The gravity
and magnetic anomaly patterns, and the observation that the gravity
low cuts across rock and age provinces, provide strong evidence that
the Missouri gravity low is a consequence of a major inhomogeneity
within the crust.

RELATIONSHIPS BETWEEN FOLDS, FAULTS, AND LINEARS
IN SOUTHERN MISSOURI AND BASEMENT STRUCTURE

In this section we describe relationships between the Missouri
gravity low and the patterns of faults, folds, and linears that
exist within the Paleozoic sedimentary rocks covering Missouri. The
particular tack that we take is to map the patterns of linear
features from HCMM thermal images, compare those linears to the
distribution of known faults and folds, and finally we relate the
trends for the structural data to the gravity low.

Figure 9 shows a HCMM thermal infrared image over southern

Missouri taken during relatively clear atmospheric conditions at approximately 1:30 p.m. on June 10, 1978. The frame has been contrast-enhanced and transformed to a Mercator projection. Water appears dark (cool) because it does not warm as quickly as vegetation, soil, or rock. A correlation plot between the apparent temperature seen in this image and a map of the magnitude of topographic slopes demonstrates that the dominate control on temperature is relief. Areas with high relief show as relatively dark (cool), while relatively flat regions are bright (warm). For instance, the bright polygonal zone centered at 37.6° N. lat., 90.5° W. long. corresponds to flat terrain underlain in part by igneous rocks of the St. Francois Mountains and in part by the surrounding Cambrian sedimentary rocks. The dark area to the southwest of this region corresponds to Ordovician carbonates that have been dissected by streams. Flood plains of the streams and the major rivers are flat and therefore relatively bright (hot). Finally, the relatively smooth, bright regions to the north of the Missouri River and east of the Mississippi River coincide with the glacial till deposits related to the Wisconsin and earlier periods of glaciation.

We also combined a shaded relief image of topography with the daytime thermal image by multiplying the two data sets on a element by element basis. The resulting product is shown in Figure 9. Clearly, linear features are enhanced in the merged data relative to either the shaded relief map or thermal images shown alone. The reasons are at least three fold. First, topographic linears can be readily discerned on shaded relief maps (Wise, 1976). Second, topographic linears associated with river valleys would be enhanced

because of the higher temperatures for the valleys as opposed to the hills. Combining the thermal image with the shaded relief map provides, in effect, a nonlinear enhancement of the topography. Third, any linear thermal features not related to topography would remain in the data. This product was used as our primary base for constructing a linears map for southern Missouri. An apparent thermal inertia image was also constructed using the formulation of Price (1977) and overlayed onto the shaded relief image. However, this product did not provide a significant amount of additional information, probably because the nightime thermal and the albedo data contain only 25% of 13% of the variance inherent in the 3 dimensional thermal day-thermal night-albedo data set.

Figure 11 is a sketch map showing linears from the processed HCMM data. Also shown are folds from a version of the Missouri structures map (McCracken 1971) and faults from the latest geologic map of the State (Anderson et al., 1979). The folds are thought to be drape folds over the Precambrian surface in areas with significant relief due to basement faulting (McCracken et al., 1971). Most of the faults are high angle normal faults, although some evidence for shear movement can be found (McCracken et al., 1971). The area occupied by the high temperature region of the St. Francois Mountains and surroundings is also drawn on Figure 11. Note that linears, faults, and folds generally strike in a direction parallel to the gravity low. Also, the sharp southwestern edge of the St. Francois Mountains is coincident with the northern flank of the low. Further away from the low the the azimuths of features tend to disperse. Clearly, the basement inhomogeneity associated

with the Missouri gravity low has had a pronounced influence on the pattern of faulting and folding that has propagated through the Paleozoic sedimentary cover. The preponderance of normal faulting in the area implies, as does the reentrant of older basement rocks along the gravity low, that the dominate structural activity associated with the crustal inhomogeneity beneath the gravity low has been one of vertical readjustment. Preferential uplift along the low is also consistent with the pattern of vertical displacements shown by the mapped faults in the area (Figure 11).

THE AGE, ORIGIN, AND EVOLUTION OF THE
MISSOURI GRAVITY LOW

The Missouri gravity low must be older than the Paleozoic sediments that have been deposited over the reentrant of older rocks into the granite-rhyolite terrain. The reason is that any uplift and stripping of the younger granite-rhyolite rocks along the gravity low must have occurred before the Precambrian surface was buried. The oldest abundant sedimentary rocks in southern Missouri consist of Upper Cambrian sandstones called the Lamotte Formation (Anderson et al., 1979).

A number of events affected the region now occupied by the gravity low during the Precambrian including: (1) The set of processes that led to formation of the granite-rhyolite terrain of southern Missouri. Bickford et al. (1981) speculate that a rifting event or a convergent plate margin might explain formation of the granite-rhyolite units; (2) Rifting that was associated with the

opening of the Reelfoot basin, the Precambrian precursor to the Mississippi embayment (Ervin and McGinnis, 1975); (3) Rifting associated with formation of the midcontinent gravity high (Chase and Gilmer, 1973); and (4) The postulated continent-continent collision associated with the Grenville orogeny (Burke and Dewey, 1973).

At this point it is useful to summarize the characteristics of the Missouri gravity low. The feature has a negative Bouguer of about 34 milligals, a width varying from 120 to 160 km, it has a medial high for part of its length, and it extends about 700 km in length. The low is perhaps best expressed within the younger granite-rhyolite terrain of southern Missouri. The flanks of the feature exhibit magnetic highs, some of which are probably due to igneous intrusions. Finally, the feature controls the pattern of normal faulting in the Precambrian basement rocks and overlying sedimentary cover. Except for the lack of a discernable thickness of sedimentary fill overlying the granite-rhyolite terrain, such a description is consistent with an origin as the failed arm of a triple junction. In fact, there are examples of relatively recent rifts that have negative anomalies with no associated sediment fill, although Burke and Whiteman (1973) interpret these anomalies as being due to ponding of magmas at the base of the crust.

The Missouri gravity low could have formed as the failed arm of a triple junction that existed before formation of the granite-rhyolite terrain. The triple junction site would have been to the southeast, with the other two rifts becoming active spreading centers. Closure of that spreading center, with subsequent

continent-continent collision, may have been the most plausible method of generating the abundant alkalic igneous activity that produced the younger granite-rhyolite terrain. In the process, most of the sediment fill within the failed rift would have been metamorphosed, intruded into, and covered by the alkalic magmas associated with formation of the granite-rhyolite terrain. The metasediments found in the reentrant of older rocks in this terrain (Figure 7) may be the remnants of this valley fill. Subsequent events, such as the formation of the Reelfoot rift that is postulated to have occurred at approximately 1.2 Ga (Ervin and McGinnis, 1975), could have served to reactivate parts of the rift. Reactivation certainly occurred during the mid-Paleozoic to Mesozoic, when the southeastern end of the low was structurally active as the Pascola arch. We stress that our interpretation, although plausible, is by no means unique and serves only as a working hypothesis to be updated or discarded as new seismic, potential field, and rock-type data are acquired. It is of interest to note that an origin as a failed rift arm may provide a new perspective on the source of the Pb-Zn-Cu in the Paleozoic sedimentary cover, since base metal mineralization is a common process associated with rifting events (Burke and Whiteman, 1973).

SUMMARY AND IMPLICATIONS

1. Standard digital image processing techniques have been used to interpolate and display free air and Bouguer anomalies and topography as gray tone, color-coded, and shaded relief images

for the midcontinent as part of an analysis of how structural features within the Precambrian basement of Missouri relate to the broader structure of the midcontinent. In addition, the Precambrian basement rock type map of Bickford et al. (1981) and magnetic anomalies for Missouri have been digitally merged and displayed with the gravity data to facilitate examination of correlations. Finally, Heat Capacity Mapping Mission (HCMM) thermal image data covering southern Missouri have been enhanced and overlayed onto shaded relief versions of topography.

2. A major and previously unrecognized gravity anomaly (Missouri gravity low) in the midcontinent is a 700 km long, 120-160 km wide free air and Bouguer low, with a Bouguer amplitude of up to 34 milligals. The anomaly displays a medial gravity high for part of its length. The low begins at a break in the midcontinent gravity high in southeastern Nebraska, extends in a southeast direction through Missouri, and intersects the Mississippi Valley graben as defined by Kane et al. (1981). The northern and southern edges of the intersection of the Missouri gravity low and the Mississippi Valley graben are the sites of discrete positive gravity anomalies that are thought to be due to plutons. Also, many of the epicenters associated with the New Madrid seismic area are within the crustal block defined by the intersection of the gravity low and the Mississippi Valley graben. Discrete positive magnetic anomalies exist along the flanks of the Missouri gravity low. Finally, the gravity low is the site of a reentrant of older Precambrian metasedimentary

rocks into the younger granites and rhyolites that underlie much
of southern Missouri. The amplitude of the low is too high to
be related to thickening of Paleozoic sedimentary rocks. Rather
the anomaly is probably due to a basement inhomogeneity. Two
seismic refraction profiles (Stewart, 1968) cut across the low
in two places in Missouri. In both cases, the seismic data are
consistent with a slightly thicker crustal section beneath the
gravity low. The magnitude of the gravity anomaly is consistent
with a crustal excess of 3.3 km as compared to surrounding areas
or with a crust that is slightly less dense (0.1 gm/cm3
contrast) in the upper 4 to 8 km.

3. A HCMM daytime thermal image was overlain onto a shaded relief
    image of topography covering the area underlain by the gravity
    low in southern Missouri. These data show that linears trend in
    the same direction as the low. On the other hand, linears tend
    to be dispersed in azimuth away from the gravity anomaly.
    Mapped faults (high angle normal faults, mainly) and drape folds
    over basement relief in the Paleozoic sedimentary cover of
    southern Missouri follow a similar pattern. Some of the HCMM
    linears correspond to the mapped structures, in some cases they
    are extensions of such features, and some linears do not
    correspond to mapped features. In any case, the correlation of
    the gravity low and the structural data suggest that the low is
    a major basement rift and that the structures in the Paleozoic
    deposits are due to vertical readjustments related to the
    crustal inhomogeneity that gives rise to the low.

4. The Missouri gravity low is older than the oldest Paleozoic
   sedimentary rocks that cover the reentrant of metasedimentary
   rocks into the younger granites and rhyolites. The oldest rocks
   correspond to the Upper Cambrian Lamotte Formation. The gravity
   low could be the present expression of a rift that formed as a
   failed arm of a triple junction occurring before or during the
   events that led to the younger granite-rhyolite terrain of
   southern Missouri. Emplacement of the igneous rocks would have
   effectively covered or metamorphosed sedimentary rocks that
   formed as valley fill with the rift. Reactivation of the rift
   has certainly taken place since it formed. Association of the
   Missouri gravity low with a unique history is difficult at this
   point because of lack of information on basement rock types,
   ages, and seismic controls on crustal configurations beneath the
   low.

ACKNOWLEDGMENT

REFERENCES CITED

Anderson, K.H., 1979, Geologic map of Missouri, Missouri Geological Survey publication, 1 sheet.

Arvidson, R.E., E.A. Guinness, J. Strebeck, G. Davies, K.J. Schulz, 1982, Image processing applied to gravity and topography data covering the continental United States, EOS, 63, 261-265.

Batson, R.M., K. Edwards, E.M. Eliason, 1975, Computer-generated shaded relief images, J. Res. U.S. Geol. Surv., 3, 401-408.

Bickford, M.E., K.L. Harrower, W.J. Hoppe, B.K. Nelson, R.L. Nusbaum, J.J. Thomas, 1981, Rb-Sr and U-Pb geochronology and distribution of rock types in the Precambrian basement of Missouri and Kansas, Geo. Soc. American Bull., 92, 323-341.

Braile, L.W., W.J. Hinze, J.L. Sexton, 1981, Ancient rift complex and related seismicity in the northern Mississippi embayment area, Geol. Soc. Am, Abs. with Programs, 13, 415.

Bretz, J.H., 1965, Geomorphic history of the Ozarks of Missouri, Missouri Geol. Survey and Water Resources, 2nd Series, 41, 134 p.

Burke, K. and A.J. Whiteman, 1973, Uplift, rifting, and break-up of Africa, in D.H. Tarling and S.K. Runcorn, eds., Implications of continental drift to the Earth Sciences, Academic Press, 735-755.

Chase, C.G. and T.H. Gilmer, 1973, Precambrian plate tectonics: The midcontinent gravity high, Earth Planet. Sci. Lett., 21, 70-78.

Cordell, L., 1979, Gravity and aeromagnetic anomalies over basement structure in the Rolla quadrangle and the S.E. Missouri lead district, Economic Geology, 67, 409-425.

Dewey, J.F. and K. Burke, 1973, Tibetan, Variscan, and Precambrian basement reactivation: Products of continental collision, J. Geology, 81, 683-692.

Eliason, E. and L.A. Soderblom, 1977, An array processing system for lunar geochemical and geophysical data, Proceed. Lunar and Planet. Sci. Conf. 8th, 1163-1170.

Ervin, C.P. and L.D. McGinnis, 1975, Reelfoot rift: Reactivited precursor to the Mississippi embayment, Geol. Soc. Am. Bull., 86, 1287-1295.

Evans, L.L., 1977, Geology of the Brushy Creek Mina, Viburnum Trend, Southeast Missouri, Economic Geology, 72, 381-390.

Gerdemann, P.E. and H.E. Meyers, 1972, Relationships of carbonate facies patterns to ore distribution and to ore genesis in the S.E. Missouri lead district, Economic Geology, 67, 426-433.

Grundmann, W.H., 1977, Geology of the Viburnum No. 27 Mine, Viburnum Trend, Southeast Missouri, Economic Geology, 72, 349-364.

Kahle, A.B. and A.R. Gillespie, and A.F.H. Goetz, 1976, Thermal inertia imaging - A new geologic mapping tool, Geophys. Res. Lett., 3, 26-28.

Kane, M.F., T.G. Hildenbrand, and J.D. Hendricks, 1981, Model for the tectonic evolution of the Mississippi embayment and its contemporay seismicity, Geology, 9, 563-568.

Kisvarsanyi, E.G., 1974, Operation basement: Buried Precambrian rocks of Missouri - Their petrography and structure, Am. Assoc. Petroleum Geologists Bull., 58, 674-684.

Kisvarsanyi, G. and E.B. Kisvarsanyi, 1976, Ortho-polygonal tectonic patterns in the exposed and buried precambrian basement of southeast Missouri, Proceedings of the First International Conf. on the New Basement Tectonics, Utah Geological Association, Pub. 5, 169-182.

Kisvarsanyi, G., 1976, Precambrian metallogenesis in the St. Francois Mtns. igneous province, S.E. Missouri, in Kisvarsanyi, E.G., ed., Studies in Precambrian geology of Missouri, Missouri Geological Survey, Rept. Inves. 61, 164-173.

Kobrick, M., 1982, Topography of the terrestrial planets, Astronomy, 10, 18-22.

McCamy K. and R.P. Meyer, 1966, Crustal results of fixed multiple shots in the Mississippi embayment, Am. Geophys. Union Monograph 10, 370-381.

McCracken, M.H., 1971, Structural Features of Missouri, Missouri Geological Survey Rept. Inv., No. 44, 68p.

McGinnis, L.D., M.G. Wolf, J.J. Kohsmann, C.P. Ervin, 1979, Regional free air anomalies and tectonic observations in the

United States, J. Geophys. Res., 34, 591-601.

Moik, J.G., 1980, Digital processing of remotely sensed images, NASA SP-431, 330 p.

Mouat, M.M. and C.W. Clendenisn, 1977, Geology of the Ozark Lead Company Mine, Viburnum Trend, Southeast Missouri, Economic Geology, 72, 398-407.

Nuttli, O.W., 1976, Seismological studies of Missouri crustal structure, in studies in Precambrian Geology of Missouri Div. Nat. Resources, Rept. Inves. 61, 184-189.

Offield, T.W., 1975, Thermal infrared images as a basis for structure mapping, Front range and adjacent plains in Colorado, Geol. Soc. Am. Bull, 86, 495-502.

Paarlberg, N.L. and L.L. Evans, 1977, Geology of the Fletcher Mine, Viburnum Trend, Southeast Missouri, Economic Geology, 72, 391-397.

Pettengill, G., E. Eliason, P. Ford, G. Loriot, H. Masursky, 1980, Pioneer-Venus radar results: Altimetry and surface processes, J. Geophys. Res., 85, 8261-8270.

Phelan, M.J., 1969, Crustal structure in the central Mississippi Valley earthquake zone, Ph.D. Dissertation, Washington University, St. Louis, Mo.

Price, J.C., 1977, Thermal inertia mapping: A new view of the Earth, J. Geophys. Res., 82, 2582-2590.

Russ, D.P., 1981, The structure of the Reelfoot rift and its relationship to some regional midcontinent features, Geol. Soc. Am., Abs. with Programs, 13, 543.

Sabins, F.F., 1969, Thermal infrared imagery and its application to structural mapping in southern California, Geol. Soc. Am. Bull., 80, 397-404.

Simpson, R.W. and R.H. Godson, 1981, Colored gravity anomaly and terrain maps of the east central United States, U.S. Geol. Survey Open-File Report 81-846.

Stauder, W., M. Kramer, G. Fischer, S. Schaeffer, and S.T. Morrissey, 1977, Seismic characteristics of southeast Missouri as indicated by a regional telemetered microearthquake array, Bull. Seism. Soc. Am., 66, 1953-1964.

Stewart, S.W., 1968, Crustal structure in Missouri by seismic refraction methods, Bull. Seismol. Soc. Amer., 58, 291-323.

Strebeck, J.W., 1982, Structure of the Precambrian basement in the Ozark plateau as inferred from gravity and remote sensing data, Masters Thesis, Washington University, St. Louis, Mo.

Sweeney, P.H., E.D. Harrison, and M. Bradley, 1977, Geology of the Magmont Mine, Viburnum Trend, Southeast Missouri, Economic Geology, 72, 365-371.

VanSchmus, W.R. and M.E. Bickford, 1981, Proterozoic chronology and evolution of the midcontinent region, North America, Chapter 11, Precambrian Plate Tectonics, A. Kromer (ed.), Elsevier Pub. Co.,

261-296.

Watson, K., 1981, Geologic applications of thermal inertia mapping from HCMM, 1981 Int. Geosci. and remote Sensing Symp., IEEE Cat. No. 81CH1656-8, 1182.

Wise, D.U., 1976, Sub-Continental sized fracture systems etched into the topography of New England, Proceedings of the First International Conf. on the New Basement Tectonics, Utah Geological Association, Pub. 5, 416-422.

Woollard, G.P., and H.R. Joesting, 1964, Bouguer gravity anomaly map of the United States, U.S. Geol. Survey.

FIGURE CAPTIONS

Figure 1 - Digital shaded relief map of topography is displayed in this image with the simulated sun located at 20° above the northeastern horizon. A Mercator projection is used for this and the other images in the paper. Numbers running vertically on the right hand side are degrees north latitude and numbers at the bottom are in degrees west longitude. The particular area of concern is located in the box bound by 25 to 49° N. lat., and 80 to 110° W. long. The resolution of the image, measured as the width of a picture element (pixel) is about 7 km. At that resolution little structural control of topography is evident within the midcontinent.

Figure 2 - Gray tone image of free air gravity anomalies for the same area as displayed in Figure 1. Black areas correspond to regions where stations were spaced too far apart to allow reasonable interpolation. Bright regions correspond to positive anomalies, medium gray to areas with anomalies close to zero, and darker areas to regions with negative anomalies. The anomaly range goes from +66 to -360 milligals. A sketch map illustrating structural features evident in the image is shown in Figure 5. The midcontinent gravity high extends as a NE-SW trending linear high, flanked by lows, in the upper half of the image. Note the subtle linear low extending from a break in the gravity high, toward the

southeast, to about 36° N. lat., 90° W. long.

Figure 3 - Shaded relief image depicting free air anomalies as if
they were hills and valleys illuminated by a sun located
at 15° above the northeastern horizon. Note the
correlation between the shaded relief of topography and
this figure in areas of high relief. Note the linear
gravity low that begins at the break in the midcontinent
gravity high and strikes southeasterly toward 36°
N. lat., 90° W. long. A Bouguer image displays a
similar patten for the linear gravity low.

Figure 4 - This color image combines a color-coded version of the
free air image shown in Figure 2 with the shaded relief
image shown in Figure 3. The effect is to be able to
discern both the value of an anomaly for a given region
and an indication of the local anomaly gradient. Red
corresponds to free air values greater than 20
milligals; yellow to orange indicate a range from 0 to
20 milligals; green corresponds to -10 to 0 milligals;
blue-green denotes -30 to -10 milligals; and blue
corresponds to values smaller than -30 milligals. This
figure was the base map used for constructing the
structural features diagram shown in Figure 5.

Figure 5 - Sketch map showing major structures delineated in the
free air images of Figures 2, 3, and 4 and equivalent
presentations for Bouguer data. The Missouri gravity
low is a subtle, but pervasive feature that extends from

the midcontinent gravity high to the Mississippi
embayment.   The location of the Mississippi Valley
graben is in part from Kane et al. (1981).   A-A' is the
location of the profiles shown in Figure 6.

Figure 6 - Topography, free air, and Bouguer anomalies are shown
for profile A-A' of Figure 5.   The profile cuts across
the Missouri gravity low.

Figure 7 - Rock types of Bickford et al. (1981) have been coded to
discrete color values and overlayed onto a shaded relief
version of Bouguer anomalies.   Sun is from the west at
15° above the horizon.   Color values are as follows:
Medium blue - felsic rocks;   yellow - granite;   orange -
rhyolite;   purple - gabbro;   dark blue - basalt;   red -
metasedimentary rocks;   green - Sioux Quartzite;   and
light blue - Keweenawan sedimentary rocks.

Figure 8 - Vertical intensity magnetic anomalies with amplitudes
greater than 600 gammas are shown as black splotches on
gray-tone and shaded relief images of Bouguer anomalies
for Missouri.   Patterns of small black splotches near
the southeastern edge of the state and in the upper
right are spurious and are remnant from the original
digitization of the Missouri magnetic anomaly map.
Arrows point to the Bloomfield (lower right) and to the
Salem magnetic highs (Phelan, 1969; Cordell, 1979).
Both features are probably due to relatively mafic
intrusions.   Note that many of the magnetic highs are

clustered on the edges of the Missouri gravity low. The sun is from the west at 15° above the horizon for the shaded relief data.

Figure 9 - This figure is HCMM daytime thermal infrared image covering southern Missouri that has been contrast enhanced and transformed to a Mercator projection. Flat areas are brighten (warmer) that regions with high relief. HCMM frame ID A-A0045-19420-2.

Figure 10 - The HCMM contrast enhanced daytime thermal infrared image has been overlayed onto a shaded relief image depicting topography. The sun for the shaded relief image is from the west at 20° above the horizon. The overlay tends to enhance subtle topographic features while retaining linear thermal anomalies not associated with relief.

Figure 11 - Sketch map showing the Missouri gravity low, mapped faults and folds, and linears as mapped from the HCMM thermal image, and from the thermal-topography overlay. The structural trend is dominated by the trend of the Missouri gravity low. Azimuths of structures tend to disperse for regions far from the low.
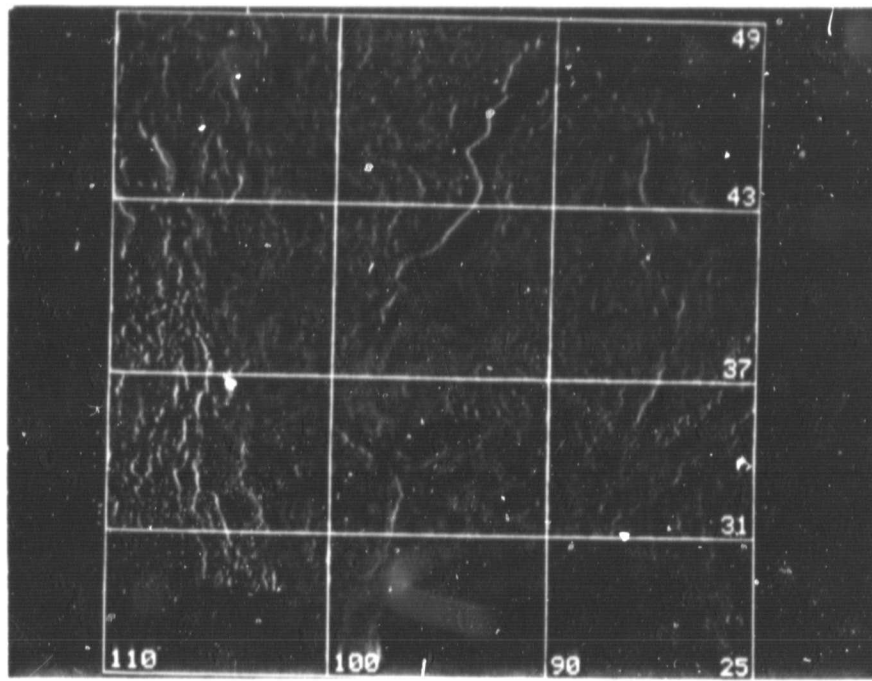
Figure 4
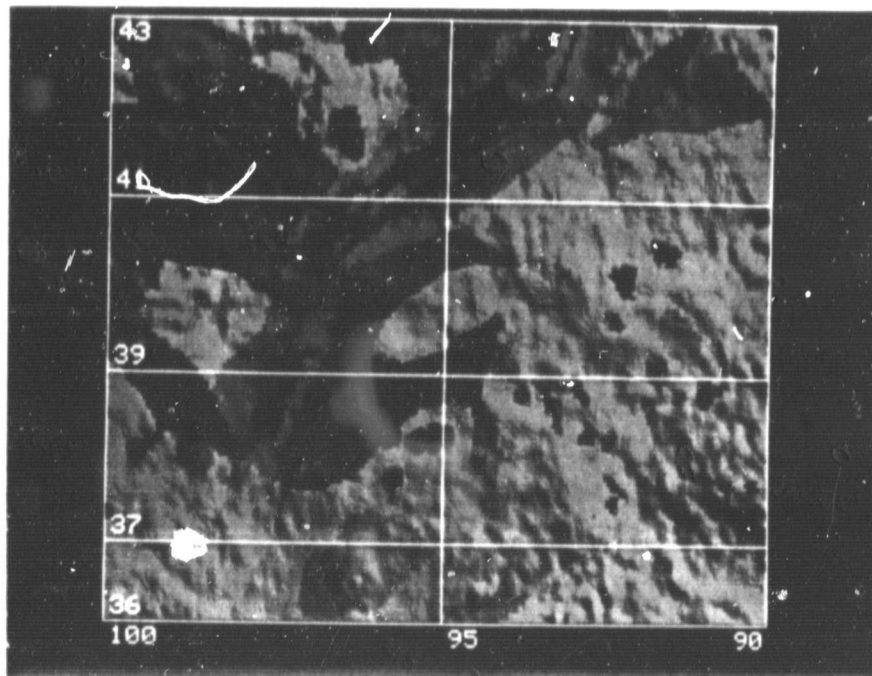
Figure 7

EOS

FREE AIR

BOUGUER

Fig. 5

TOPOGRAPHY

FREE AIR

BOUGUER

A

A'

DISTANCE, km

0   100   200   300

kilometers

0.3   0.2   0.1

mgals

20   10   0   -10   -20   -30   -40

HCMM DAY-IR
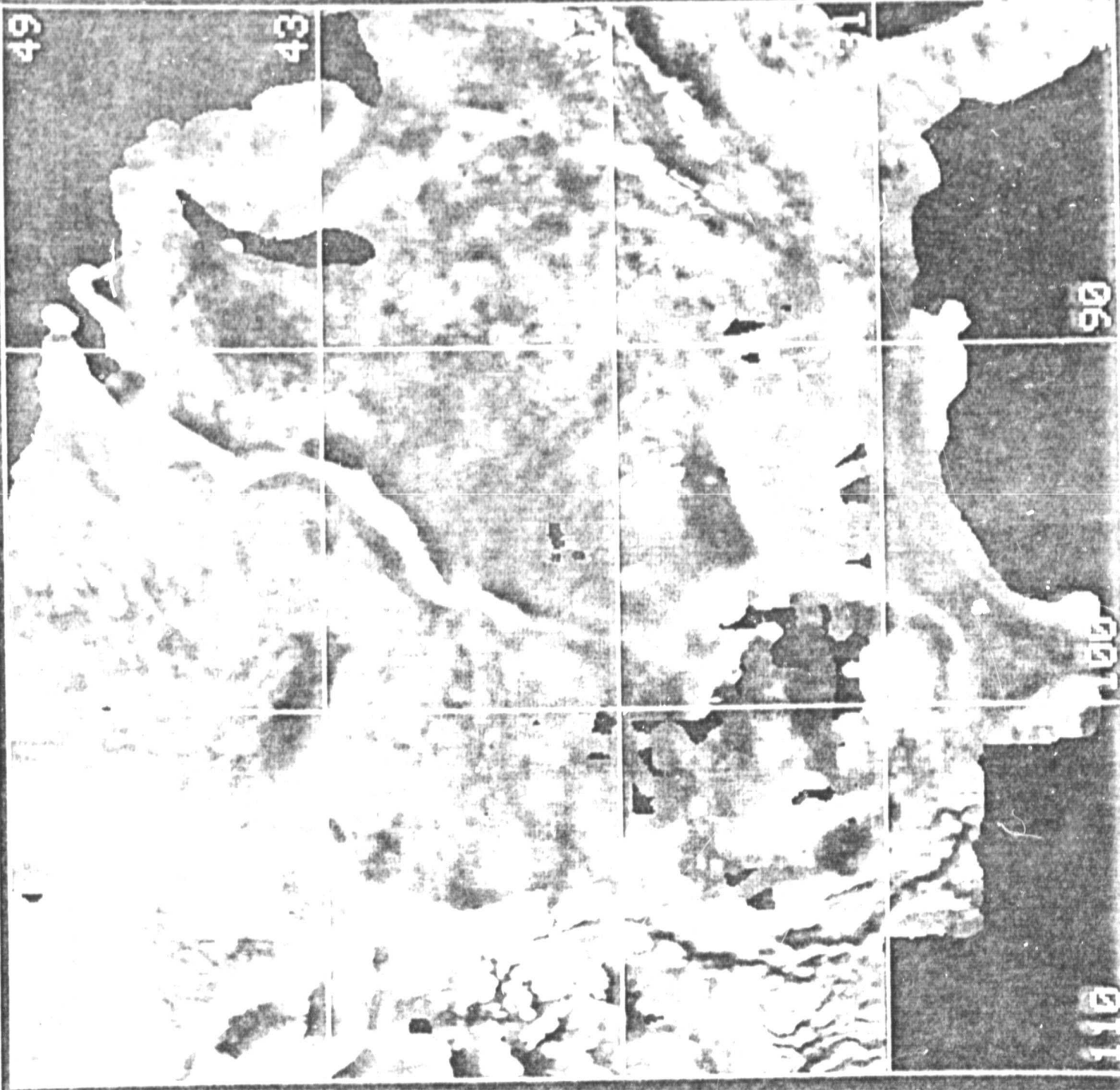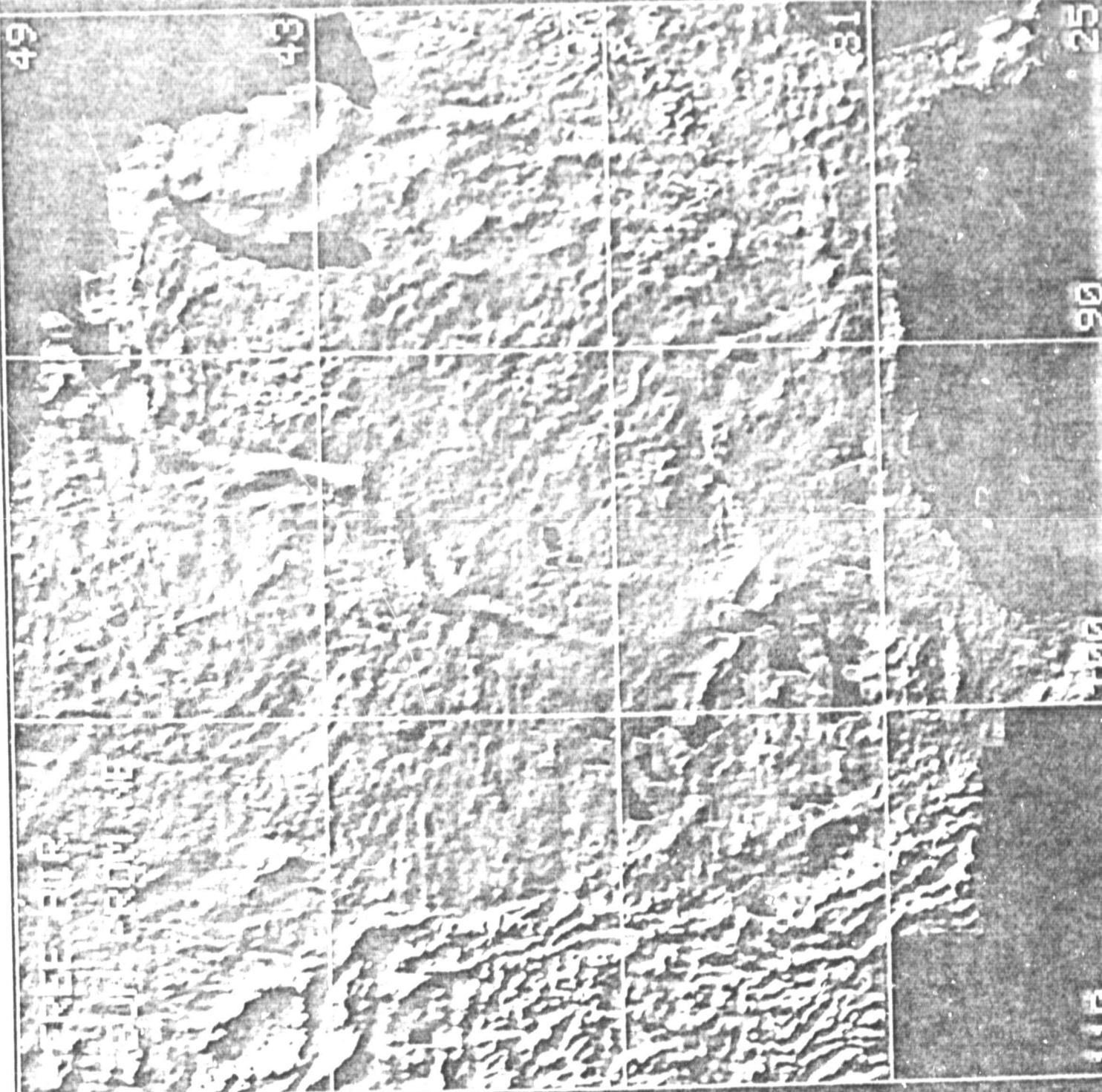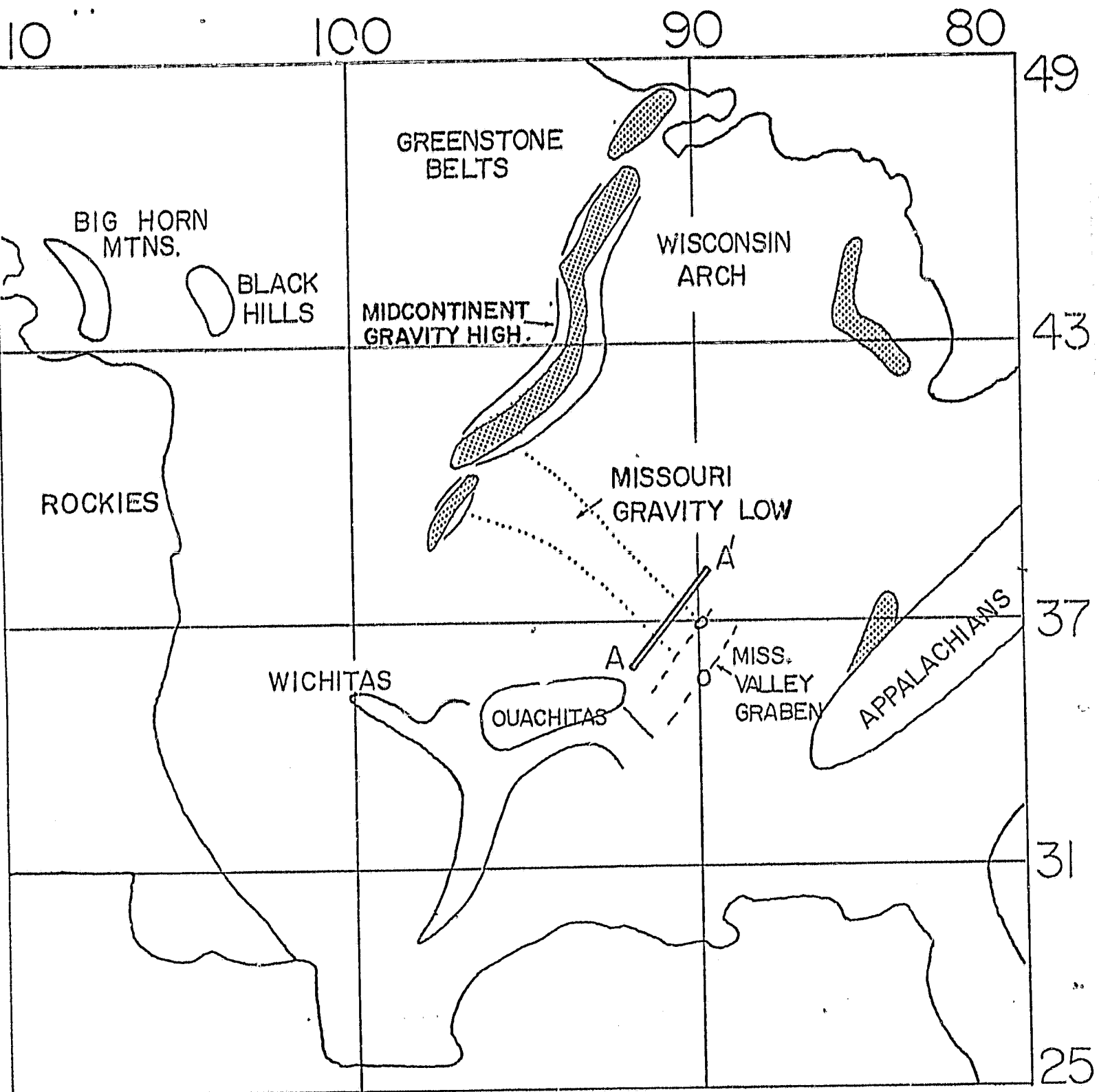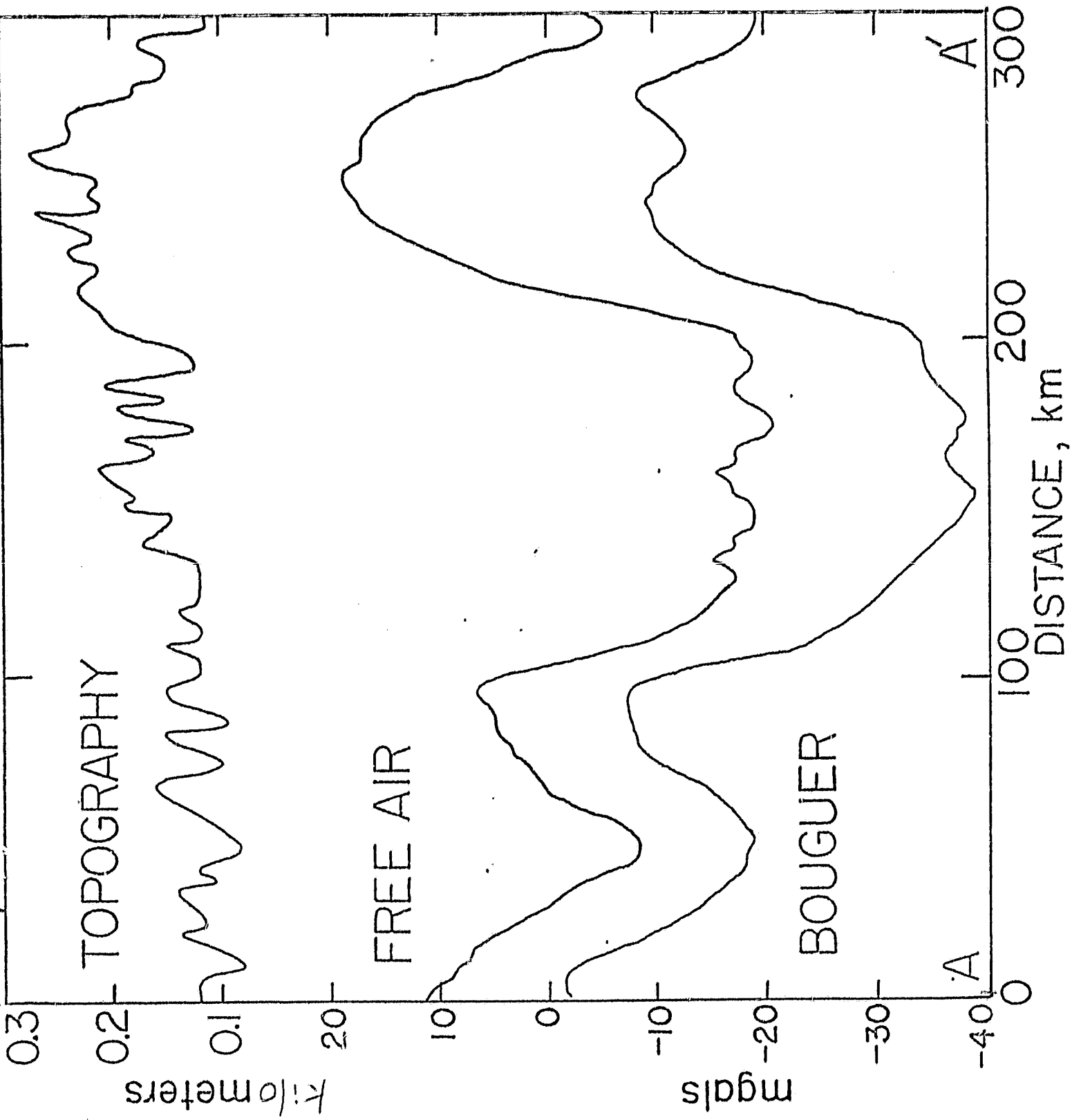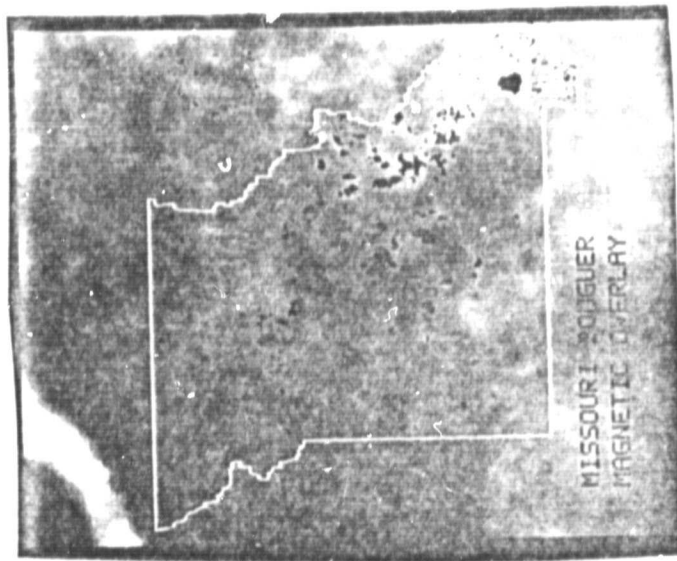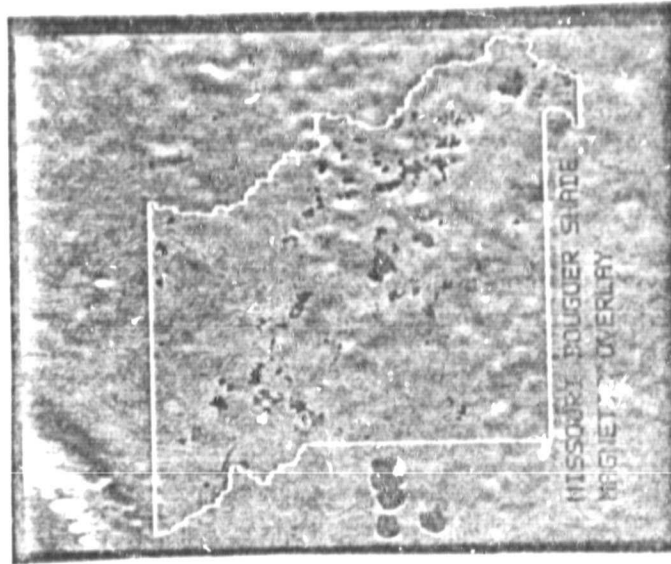
Fig. 9
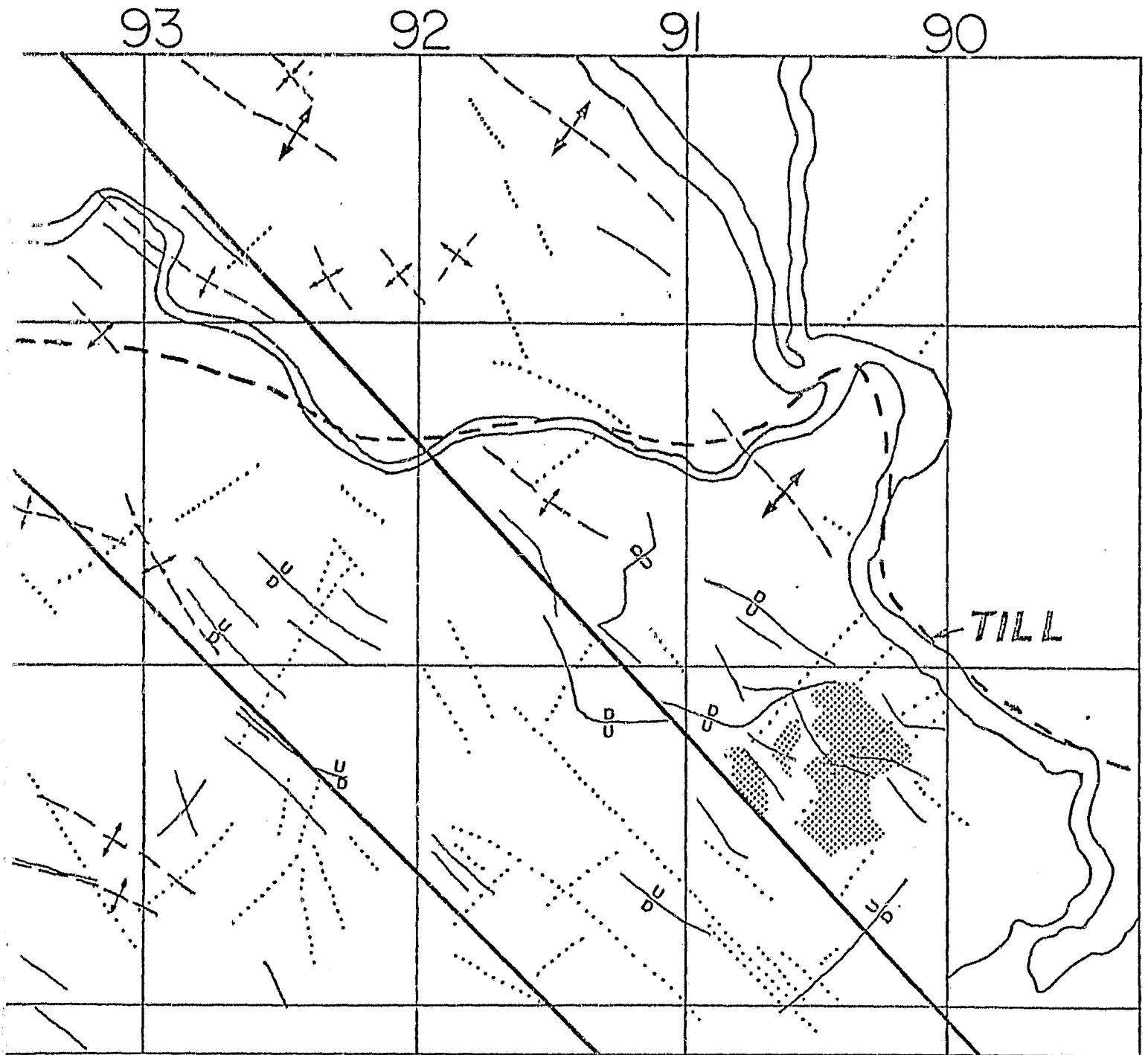
Fig. 11
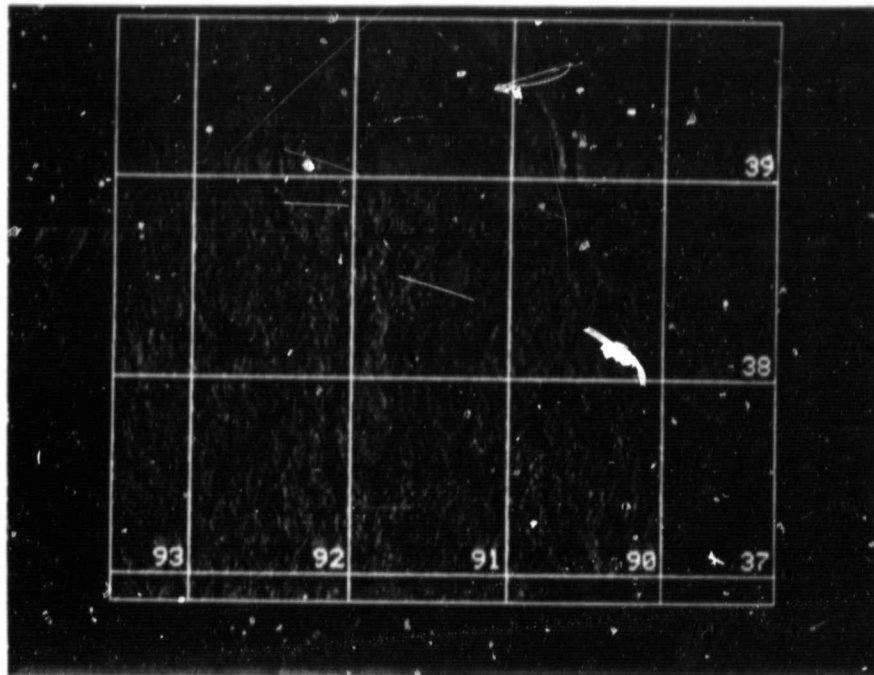
HCMM Apparent thermal inertia has been color coded and overlain onto a shaded relief map depicting topography. Reds correspond to high A.T.I., blues to low values.
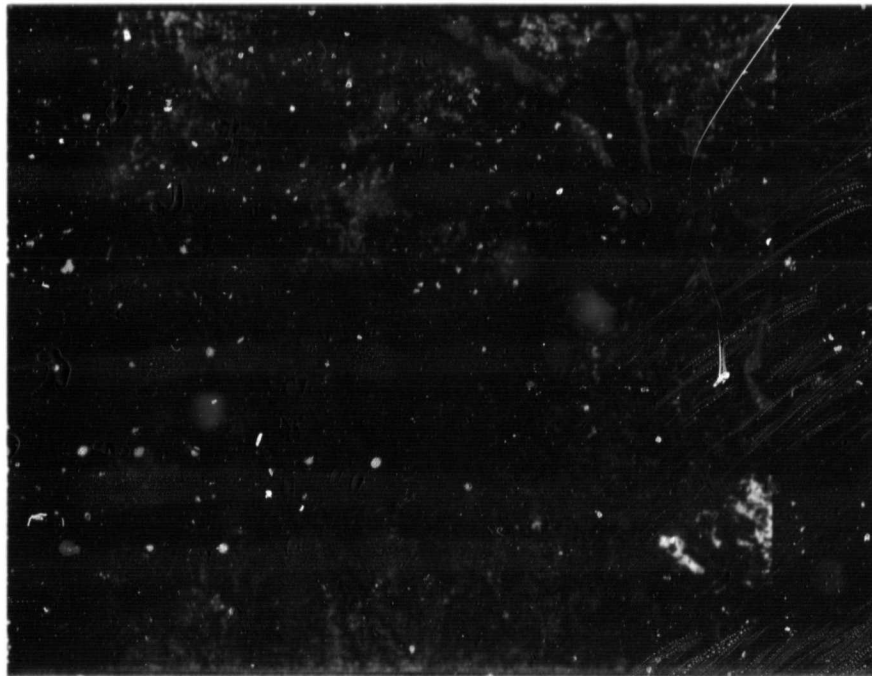
HCMM daytime thermal infrared brightness is coded as hue, albedo as saturation, and nighttime thermal infrared as intensity. Reds indicate relatively high values of daytime temperature.

OF POOR QUALITY

The case is then made that the shock wave results reported by Brown and MacQueen, who reported the ε-γ phase transition at 200 GPa, favor the choice of γ-iron at inner core pressures.

It appears that pure γ-iron alone satisfies the density and bulk modulus requirements of the inner core. Geochemical arguments would favor the addition of Ni to pure iron. However if Ni is added to γ-iron, a lighter element (such as S) must also be added to compensate for the increase in density resulting from the Ni.

T21A-9

New Shock Wave Data for Pyrite and its Relation to the Earth's Core

THOMAS J. AHRENS and CHRISTOPHER R. CREAVEN* (Seismological Laboratory, California Institute of Technology, Pasadena, CA 91125) (*Present address: Atlantic-Richfield Corp., Los Angeles, CA)

New shock and release wave data in the 73 to 1830 kbar range for single crystal pyrite (Fe^{+2}, low spin) demonstrate no detectible phase change, over the pressure range investigated. Combining the present data with Simakov et al. data to 3200 kbar, fits closely to linear shock (U_s) particle (U_p) velocity relation U_s(km/sec) = 5.36 + 1.44 u_p. The inferred zero-pressure bulk sound speed is close to that observed ultrasonically; 5.36 to 5.43 km/sec and the release data constrain the sound speed along the Hugoniot to lie in the range 5.0 to 6.2 km/sec from 384 to 1830 kbar, and constrain the density variation of Gruneisen ratio to γ ≈ 3.8 $(\rho_0/\rho)^{1.3}$. This behavior contrasts markedly with that of Fe$_{0.9}$S which initially has Fe^{+2} in the high-spin state and undergoes an ~14% density increase to a high pressure phase below 100 kbar, which may have Fe^{+2} in the low-spin state. When the new pyrite data and recent reanalyses of pyrrhotite are used with shock wave data for iron and seismic data for the core the essentially nearly ideal additivity of the molar volume of S in iron sulfides can be demonstrated. Depending on thermal profiles assumed, some 9 to 13 and 10 to 13% S are inferred in the liquid outer core from the pyrite and pyrrhotite data, respectively.

T21A-10

Dynamics of Chemically Enriched, Internally Heated Plumes in the Mantle

Henry E. Eby and David A. Yuen (Dept. of Geology, Arizona State University, Tempe, AZ 85287)

It has been proposed that plumes are finite-amplitude manifestations of localized thermal instabilities produced at the lower (hot) thermal boundary layer, owing to the destabilizing effects of strongly temperature-dependent mantle rheology. If the primitive deep mantle is enriched in radioactive heat sources from inhomogeneous planetary accretion (Anderson, 1975), then thermal instabilities may furnish a viable mechanism to extract the enriched heat sources into the upwelling, which is then propelled rapidly upwards by these moving heat sources. Accordingly we have modelled the thermal-mechanical structures of these chemically enriched, subsolidus plumes by means of boundary layer techniques in which both internal heating with a localized spatial variation and a strongly temperature-dependent viscosity, characteristic of mantle materials, are incorporated. The equations governing the conservation of mass, energy and momentum are solved numerically. Two different modes of heating have been studied: (a) the plume is driven solely by a concentrated amount of radiogenic heating (b) the energy source is derived from both the localized radioactivities and a hot adiabatic temperature imposed at the centerline of the plume. We find that for mechanism (a) to produce velocities greater than 10 cm/yr requires radioactive concentrations equivalent to those typical of granitic rocks. On the other hand, narrow, fast mantle plumes, 0 (m/yr), are easily achievable for heat production rates characteristic of oceanic basalts and adiabatic temperature excesses of a few hundreds of degrees.

Anderson, D.L., Chemical Plumes in the Mantle, Geol. Soc. America Bull., 86, 1593-1600, 1975.

T21A-11

Time-Dependent Numerical Models of Single and Double-Layer Mantle Convection

A. P. BOSS and I. S. SACKS (Dept. of Terrestrial Magnetism, Carnegie Institution of Washington, 5241 Broad Branch Road NW, Washington DC 20015)

Contrary to geochemical evidence, current models of mantle convection assuming steady state motion favor single-layer convection. Relaxing the steady state assumption, we have studied the time evolution of two-dimensional Boussinesq convection. A survey involving variation of several parameters has been completed. Each model has Cartesian geometry, exponential viscosity dependence on temperature, and free-slip boundaries. Initial conditions were chosen as a fluid at rest with a uniform temperature gradient (pure conduction), randomly perturbed (the 5% level). Parameters varied include: choice of initial noise, Ra (10^5 to 10^6), aspect ratio A (1 to 2), heating source (all bottom, all internal, or half and half), and spatial variation in the temperature along the bottom boundary (25% amplitude cosine variation).

The time development is sensitive to the choice of the initial noise, except when variations in the bottom temperature are present, which then determine the transient cell structure (plumes rise over each temperature maximum). For Ra=10^7, the initial single-layer structure forms a transient phase of double-layer convection, with as many as 4 cells in each layer. Steady state solutions in all cases favor single-layer convection. Increasing A increases the tendency for the double-layer transient to occur. Varying the location of the heat source has little qualitative effect upon the evolution. Double-layer structure occurs without the large temperature difference between the two layers required in steady state.

The timescale for existence of the double-layer structure is 1 b.y. (with Ra=10^7, as appropriate for whole-mantle convection). When compared to the timescale for plate motions (about 0.1 b.y.), the results imply that time-dependent models are necessary for understanding mantle convection; transient periods of double-layer convection may have existed in the past, or may exist now.

CONTINENTAL GEOPHYSICS
(FP) Dominion C Tues AM
Larry Brown (Cornell Univ)

Presiding

T21B-1

Gravitationally Induced Stresses in a Thin, Spherical Shell

A. K. GOODACRE (Division of Gravity, Geothermics and Geodynamics, Earth Physics Branch, Ottawa, Ontario, K1A 0Y3)

In situ stress measurements generally indicate that the vertical compressive stress is zero at the surface of the Earth and increases with depth approximately as the overburden pressure. On the other hand, the mean horizontal compressive stress is non-zero (≈10 MPa) at the surface and increases with depth less quickly than the overburden pressure does. The result is that the ratio of horizontal to vertical stress is greater than unity near the surface and only tends to fall below unity at depths greater than 1 to 2 km. This behaviour (in particular the presence of non-zero horizontal compressive stresses at the surface) is predicted for gravitationally induced stresses in a thin, homogeneous, elastic spherical shell enclosing a "fluid" under a pressure equal to the total weight per unit area of the shell. The horizontal compressive stress at the surface is related to the thickness of the shell. Assuming that only a thin portion of the Earth's outer crust can sustain shear stresses over long periods of geologic time, data from Canada and southern Africa indicate that the effective thickness of the elastic crust in these areas is of the order of 4 and 2 km respectively. Although two-dimensional elastic theory does not predict finite horizontal compressive stresses at the Earth's surface, the results of the thin shell theory can be used to help correct the calculations of gravitationally induced stresses in simple two-dimensional geological models.

T21B-2

New Depth-to-Curie Isotherm Map of Arizona

M. R. Hong (Center for Lithospheric Studies, The University of Texas at Dallas, Richardson, Texas 75080)
C. L. V. Aiken (same)
W. J. Peeples (Department of Geological Sciences, The University of Texas at El Paso, El Paso, Texas 79968)

The variation in heat flow in Arizona has been interpreted utilizing a variety of geophysical and geochemical data. The depth-to-Curie isotherm has been previously determined in Arizona by spectral analysis, spectral matching, and by examining the general amplitude variations of aeromagnetic anomalies. There are significant disagreements between the interpretations of much of these data. In this study, the Curie depth has been analyzed by inversion of over 60 magnetic anomalies, with the Backus-Gilbert technique providing statistical analysis of the results. Vertical resolution is ±2 km at 20 km. Depths range from 5 km below sea level to 21 km b.s.l. The results agree in general with spectral matching results, but not well with the other types of Curie depth analyses. Shallow depths are indicated along the transition between the Colorado Plateau and Basin and Range provinces, in the White Mts., in southwest Arizona, and in southeast (Tucson area) Arizona. Central and south-central Arizona in the Basin and Range show anomalously deep (20 km) Curie depths. An assumption is made that the thickness of magnetic bodies is determined thermally, not lithologically. Although the lateral variation in heat flow measurements generally agree with lateral changes in Curie depths, few completely corrected values are available. Some correlations exist with crustal seismology experiments. Preliminary MT modeling by M. A. Ander of Los Alamos National Laboratory indicates extremely close correlations with relative variations of Curie depths in various parts of Arizona. Numerical heat flow models using the Curie temperature as a boundary condition have been constructed to compare with heat flow and MT interpretations.

T21B-3

Linear Basement Structure in the Midcontinent, U.S.A. - Gravity, topography, remote sensing, and seismicity data.

R.E. ARVIDSON, E.A. GUINNESS, J.W. STREBECK (McDonnell Center for the Space Sciences, Washington University, St. Louis, Mo., 63130)

Some 500,000 individual gravity readings for the continental U.S. were reduced to free air and Bouguer anomalies. The anomalies were then filtered to produce maps with 256 contour intervals using the algorithm that generated the Pioneer Venus altimetry maps. A linear gravity low, with an amplitude of about 30 mg, extends from a break in the midcontinent gravity high in S.E. Nebraska to the Pascola Arch (horst) in the Mississippi Embayment. There is a suggestion of an extension to the northwest into Wyoming based on (1) The alignment of a sharp gradient (but only a few mg Δ) in the free air data along the North Platte River, and (2) The alignment of fractures in the Precambrian of Wyoming. In southern Missouri, as shown by digital topography and Heat Capacity Mapping Mission data, the gravity low seems to have controlled a number of basement normal faults. In addition, most of the New Madrid seismic epicenters occur in the crustal block defined by the intersection of the low with the Mississippi Valley graben. The origin of this linear basement structure is problematical, although the fact that the structure cuts across age and province boundaries is suggestive of a transcurrent fault.

T21B-4

Linear Structures in Missouri Seen with Heat Capacity Mapping Mission (HCMM) Data

J.W. STREBECK, E.A. GUINNESS, R.E. ARVIDSON (McDonnell Center for the Space Sciences, Washington University, St. Louis, Mo., 63130)

An apparent thermal inertia map was produced for the state of Missouri using HCMM night/day thermal infrared (IR) images and an albedo image. Differences in rock types (between Precambrian igneous rocks, Cambrian section, and younger units) and some structural linear features can be seen on the map. These structures were emphasized by overlaying the thermal inertia images on digital shaded relief maps depicting topography. In general, there is a good correspondence between structures seen in the HCMM data and mapped faults. Often, HCMM structures extend beyond limits of mapped features. In addition, a number of natural linear features were detected that do not correspond with mapped structures. Finally, the observed trend of many of the HCMM structures is coincident with a 30 mgal, 140 km wide, Bouguer gravity low that traverses Missouri in a NW-SE

This page may be freely copied.

Image Processing Applied to Gravity and Topography Data Covering the Continental U.S.

R. E. Arvidson, E. A. Guinness, J. W. Strebeck, G. F. Davies, and K. J. Schulz

McDonnell Center for the Space Sciences
Washington University
St. Louis, Missouri

Introduction

A great deal of digital topographic information and gravity data exist that cover the continental United States. For instance, data sets that can be purchased from the National Oceanic and Atmospheric Administration (NOAA) include (a) elevations averaged over 30 s of latitude and longitude for the coterminus United States and (b) over a half million gravity readings from stations distributed across the entire country, although in an irregular manner. Both the topography and the gravity data sets are fundamental to the understanding of the structure of the crust and lithosphere, and especially to the understanding of the relationships between topography and structure [*McGinnis et al.*, 1979; *McNutt*, 1981; and others].

The intent of this work is to show the applicability of fairly standard image-processing techniques to processing and analyzing large geologic data sets. In particular we have utilized image-filtering techniques to interpolate between gravity station locations in order to produce a regularly spaced data array that preserves detail in areas with good coverage and that produces a continuous tone image rather than a contour map. We have used standard image-processing techniques to digitally register and overlay topographic and gravity data, and we have displayed the data in ways that emphasize subtle but pervasive structural features. In this paper we discuss the techniques used, briefly describe the products, and illustrate the potential of the methods by discussing subtle linear structures that appear in the processed data between the midcontinent gravity high and the Appalachians.

Data Processing Techniques

Data processing was conducted on a PDP-11/34 minicomputer with interactive image storage and display peripherals. Software is based on mini-VICAR, with a variety of applications programs to conduct filtering, enhancement, and geometric operations. The reader is referred to such standard references as *Moik* [1980] for further information about general techniques used in image processing. Our software was developed partly at the Jet Propulsion Laboratory; partly at the U.S. Geological Survey, Flagstaff, Arizona; and partly by us.

For purposes of this paper the dynamic range of both the topography and the gravity data were first scaled to fit within the range occupied by a byte variable (i.e., 8 bits or 256 discrete values). The byte-encoded data were then stored in data arrays, where the array element spacing was 30 s in both latitude and longitude. For the topography this procedure produced a regular array of byte-encoded

data that had 2880 rows (latitude) and 7080 columns (longitude). The data arrays covered a latitude range from $25°$ to $49°N$ and a longitude range from $66°$ to $125°W$.

The resulting topography data array could be displayed as an image if the byte-encoded data were converted to color or brightness values. An alternative and quite useful method of depicting topography is to generate a digital, shaded relief map. Figure 1 shows such a product, which was generated on a version of the data file that was first transformed to a Mercator projection, digitally reduced in size by a factor of 7, and then used to generate a relief map. The shading process is based on the assumption of a photometric function for the surface (Lommel Seeliger function in our case). The brightness assigned to a given array element location depends on the local slope magnitude and direction and is relative to an assumed solar azimuth and elevation [*Batson et al.*, 1975].

The gravity data were reduced to Free air and to Bouguer anomalies courtesy of the Geopositional Department, Defense Mapping Aerospace Agency Center, St. Louis, Missouri. The reference field at sea level that was used in the reduction was based on the 1967 International Gravity Formula, with all the data referenced to the 1971 International Gravity Standardization Net. Free air anomalies were computed from the following formulation: $\Delta g_{FA} = g + 0.3086h - \gamma$, where Δg_{FA} = Free air anomaly (mGal), g = reading, h = elevation (positive down to geoid), and γ = theoretical gravity value. A second-order term was added to the elevation correction when the magnitude of the correction exceeded 0.1 mGal. Bouguer anomalies were computed on the basis of a slab with density 2.67 gm/cm^3, using $\Delta g_{BA} = \Delta g_{FA} - 0.1119h$, where Δg_{BA} = Bouguer anomaly in mGal. Local terrain corrections were not included in the Bouguer anomaly computations.

Generating images from the gravity data presents a more complicated problem than the topographic data since the gravity stations are not located along a regular grid. For both the Free air and Bouguer anomalies the data were first scaled to fit within a byte variable (i.e., 256 discrete values). The scaled data
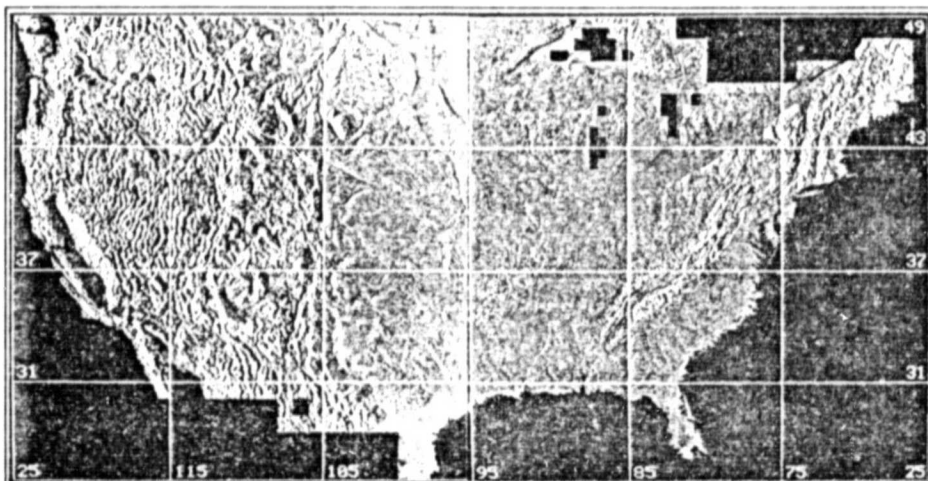

Fig. 1. Shaded relief map depicting NOAA 30-s elevation averages for the continental United States. Numbers running vertically along the sides of the image are degrees of north latitude, while numbers along the bottom are degrees of west longitude. This and other maps in the paper are Mercator projections. The simulated sun was set at 20° above the western horizon. Dark blocky areas are missing data.

were placed into an array with the same element spacing (30 s) and geographic coverage as the topography data array. The element location closest to a given gravity station location was assigned the station value, thereby producing an array occupied in part by real data and in part by blank zones.

We chose to use a conceptually simple, but powerful, filtering approach for interpolating between the real gravity data points. The technique was developed for processing lunar consortium data and was also used to produce altimetry maps from the approximately 100,000 elevation estimates obtained by the Pioneer Venus radar mapper [Eliason and Soderblom, 1977; Pettengill et al., 1980]. The technique involves use of a spatial filter that generates a moving average through the data array. At any given postion within the data array the filter occupies a box of $N \times N$ elements. The mean value of the gravity anomalies for stations located within the box is used as the interpolated value for the box center only if an anomaly value does not already exist at that location. Shifting the filter over the array and repeating the operation for each element location results in a partially interpolated data set. Blank areas still remain in zones without any data and in zones with so little data that a user-defined statistical threshold was not met. The threshold is defined in terms of the fraction of elements within the box that must have valid data in order to replace the midpoint element with the average, assuming that the midpoint did not already have valid data.

In practice the gravity data were processed by using several filter widths, beginning with a 3×3 element filter and ending with a 21
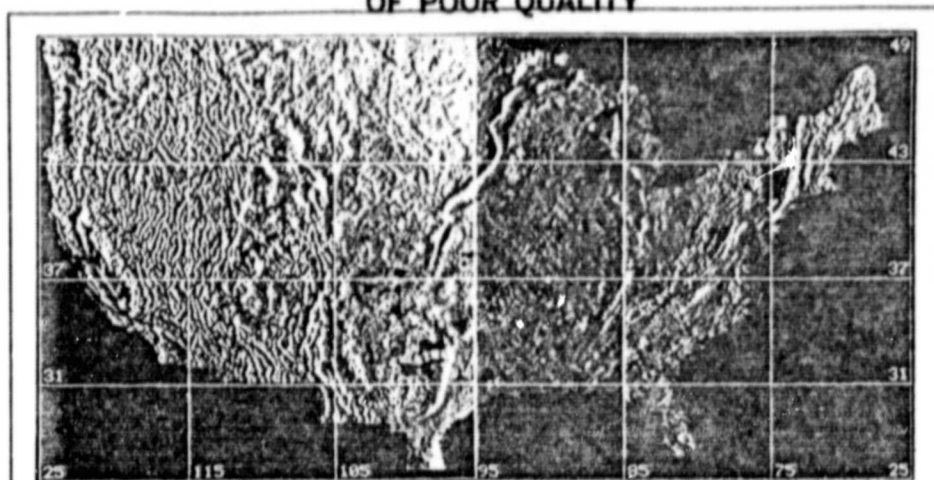
Fig. 2. Shaded relief map depicting filtered Free air anomalies. Black areas indicate regions containing either bad data or too little data to have statistically valid interpolations. The simulated sun was set at 15° above the western horizon. Variations in the anomalies are, in effect, illuminated as if they were a set of topographic ridges and valleys. For example, the midcontinent gravity high (43°N, 94°W), which is a positive anomaly, stands as a ridge, while the great valley of California (37°N, 120°W), which is a negative anomaly, appears as a trough.

$\times$ 21 element filter. The threshold was set such that at least 20% of the element locations at any given filter position must have had real data values to be interpolated. The choice of filter sizes was governed by the station spacings, which averaged several kilometers but varied from hundreds of meters to several tens of kilometers. A 3×3 element filter, for instance, covers 90 s of arc in both latitude and longitude, or about 3 km along a

line of latitude. Note that regions with relatively small distances between gravity values were interpolated only over relatively short distances, since once an element was assigned a data value it was not affected by later filter passes. The net effect of the filtering operations was to generate a regular array of gravity data, with original data left intact and with interpolated data between the original values. Some areas in the array, even with a 21×21 element filter, still had too little data to allow interpolation. Those areas appear black in all of our displays.

The filtered gravity anomalies could be displayed as gray tone or as color-coded images. As with topography, we find that a very effective visual display is a shaded relief map. Figures 2 and 3 depict shaded relief maps for the Free air and Bouguer anomalies, respectively. Comparison of these products with previously published contour maps [e.g., Woolard and Joesting, 1964; McGinnis et al., 1979] show similar broad-scale patterns. However, the maps shown in Figures 2 and 3 display inherently more information. The reasons are threefold. First, a finer grid spacing was used to interpolate between station readings than any published map we have been able to examine. Second, there are as many contour intervals as there are values in a byte variable (i.e., 256). Most contour maps typically have a dozen or so contour intervals. Third, areas with a large number of closely spaced stations retain details of the anomaly patterns.

The filtered gravity anomalies can also be digitally overlayed onto the topography for a visual display of the correlations between the two variables. The technique that we used was to first convert the byte value for each element in the gravity arrays to a given color (Figure 4). The colors were chosen in such a manner that blue corresponded to the most negative anomalies and red to the most positive anomalies. Oranges, yellows, and greens were chosen to represent intermediate values. Color-coded images depicting the anomaly patterns were digitally overlayed onto a shaded relief map of the topography simply by re-

All of the authors are with the Department of Earth and Planetary Sciences, Washington University. Raymond E. Arvidson *(far right) is an associate professor and received his Ph.D. from Brown University in 1974. He has been involved in planetary research and remote sensing for about a decade, including serving as team leader for the Viking Lander Imaging Team. He is currently a member of the National Academy of Sciences' Space Science Board and chairman of the board's Committee on Computation and Data Management. He is also an associate editor of JGR.*

Edward A. Guinness *(far left) received his Ph.D. in 1980 in planetary geology from Washington University and is now a senior scientist at the university's McDonnell Center for the Space Sciences. He spent a total of a year at the Jet Propulsion Laboratory, participating in the Viking mission operations. Guinness did his thesis research on the spectrophotometric properties of Martian surface materials, based on lander imaging data. He is continuing those studies, using data received from direct links from the Mutch Memorial Station (Viking Lander 1).*

John W. Strebeck *(second from right) received his master's degree from Washington University in 1982. His thesis topic involved geological and geophysical interpretations of the Missouri gravity low, a feature discussed in this paper. Strebeck is currently employed by Mobil Exploration Services, Inc., Dallas, Texas.*

Geoffrey F. Davies *(middle) is an associate professor and received his Ph.D. in 1972 from the California Institute of Technology. His research interest range from thermal evolution histories of the earth and planets to mantle convection and the tectonic evolution of continents. He has served on NASA advisory panels and is an associate editor of JGR.*

Klaus J. Schulz *(second from left) is an assistant professor and received his Ph.D. in petrology from the University of Minnesota in 1977. His interests range from the petrogenesis of the early continental crust to the effects that large impact events had on the subsequent thermal and tectonic regime of the earth's early lithosphere. Schulz will join the U.S. Geological Survey, Reston, Virginia, in June 1982.*
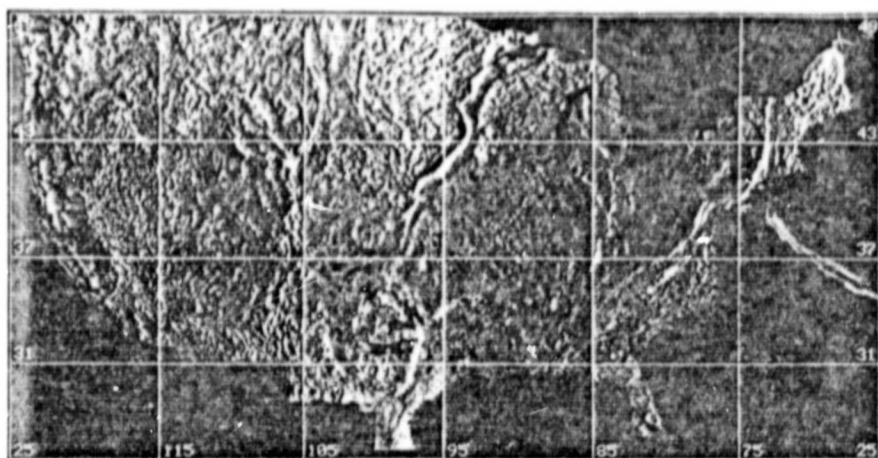
Fig. 3. Shaded relief map depicting filtered Bouguer anomalies. The map was produced in the same manner as the Free air anomaly map in Figure 2. No local terrain corrections were included in computing Bouguer anomalies.
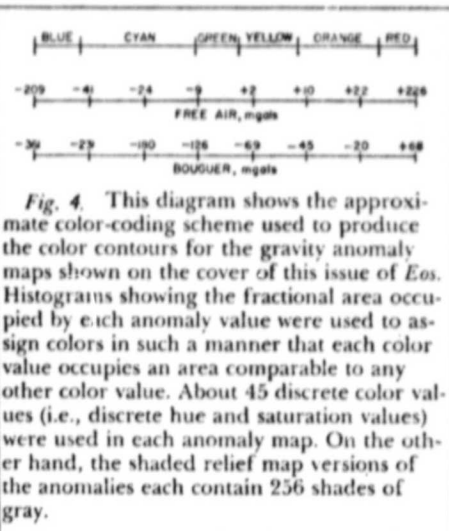

Fig. 4. This diagram shows the approximate color-coding scheme used to produce the color contours for the gravity anomaly maps shown on the cover of this issue of *Eos*. Histograms showing the fractional area occupied by each anomaly value were used to assign colors in such a manner that each color value occupies an area comparable to any other color value. About 45 discrete color values (i.e., discrete hue and saturation values) were used in each anomaly map. On the other hand, the shaded relief map versions of the anomalies each contain 256 shades of gray.

placing the brightness component for each color with the brightness from the corresponding location in an array containing the shaded relief map. The net result is a color map where the brightness is modulated by the shaded relief map, while the color hue (dominant wavelength) and saturation (degree of purity) are controlled by the gravity anomaly values. Note that any color can be uniquely defined by a hue (dominant wavelength), saturation (purity), and brightness [*Slater*, 1975]. Such products are shown for both the filtered Free air and Bouguer anomalies on the cover of this issue of *Eos*. In both cases the maps were transformed to a Mercator projection, digitally reduced by a factor of 7, and then processed as discussed above.

Discussion

A sketch map showing some of the major structures evident in the color and shaded relief maps is shown in Figure 5. For this paper we will restrict our discussion of the processed data to a portion of the midcontinent, where we have a continuing interest in the crustal structure and the relationships between basement fractures and ore deposits. Such a discussion also serves to illustrate the kinds of information that can be gleaned from topography and gravity data that have been processed in image format.

The dashed lines in Figure 5 define two major structures in the midcontinent: a newly discovered feature we call the Missouri gravity low and the Mississippi Valley graben, as defined by *Kane et al.* [1981] on the basis of gravity and aeromagnetic anomalies. The

Geophysical Prospecting

Geophysical Journal of the Royal Astronomical Society

Blackwell Scientific Publications

Missouri gravity low can be seen on the color and shaded relief maps as a 140-km-wide feature that begins at a break near the southern edge of the midcontinent gravity high and extends across Missouri and into the Mississippi embayment. In the embayment the low takes the form of a horst block called the Pascola Arch [Ervin and McGinnis, 1975]. The low has a Bouguer amplitude of about 30 mGal for the region just to the northwest of the embayment. The magnitude of the anomaly suggests a deep basement structure. In fact the anomaly is consistent with an increased crustal thickness of 3 km at the Moho or with a crust that has a density of 0.1 gm/cm^3 less than the surrounding areas for the first 4 to 8 km below the surface [Strebeck, 1982]. Analyses of remote sensing data and ground studies for areas overlying the gravity low demonstrate that the regional fracture trends are coincident with the strike of this deep basement feature, suggesting a fair degree of control over the pattern of faulting in the area [Guinness et al., 1982].

The intersection of the Missouri gravity low and the Mississippi Valley graben has clearly served to control the emplacement of two mafic plutons defined by Hildenbrand et al. [1977]: the Bloomington intrusion to the north and the Covington intrusion to the south. The two plutons can be seen as positive anomalies in the Free air color map and as bumps on the shaded relief maps. Additionally, Figure 6 is a gray tone image of the filtered Free air data that has been contrast enhanced to show the variations in the midcontinent. In such a display the most negative anomalies are dark, and less negative anomalies are bright. The Missouri gravity low is clearly discernible, and there is a suggestion of a NE-SW trending structure that, in fact, outlines the Mississippi Valley graben. The white dots represent over 1000 earthquake epicenters recorded by the St. Louis University seismic network between 1974 and 1979 [Stauder et al., 1977]. Clearly, the epicenters, which delineate the New Madrid seismicity high, are concentrated in the crustal block defined by the intersection of the Missouri gravity low and the Mississippi Valley graben. Thus the intersection of these two crustal structures seems to have provided both a zone of weakness for the emplacement of plutons and a focus for release of strain energy via earthquakes.

Examination of the Free air color map suggests an extension of the Missouri gravity low from the midcontinent gravity high to the northwest, perhaps as far as to the Big Horn uplift in Wyoming. The suggestion is based on an alignment of a sharp break in the Free air anomalies with the North Platte River valley in Nebraska and with fractures in Wyoming. The reality of such an extension must remain open to question until further study. If the extension is genetically related to the Missouri gravity low, the combined lengths of the two features would be over 1500 km. There are other structures of comparable length on the earth, namely transcurrent faults such as the Altyn Tagh of China [Molnar and Tapponier, 1975]. It is conceivable that the Missouri gravity low and the extension into Wyoming are part of a transcurrent fault system, sections of which have been reactivated during various time periods. Such an origin is also consistent with the observation that the structure cuts across the basement age
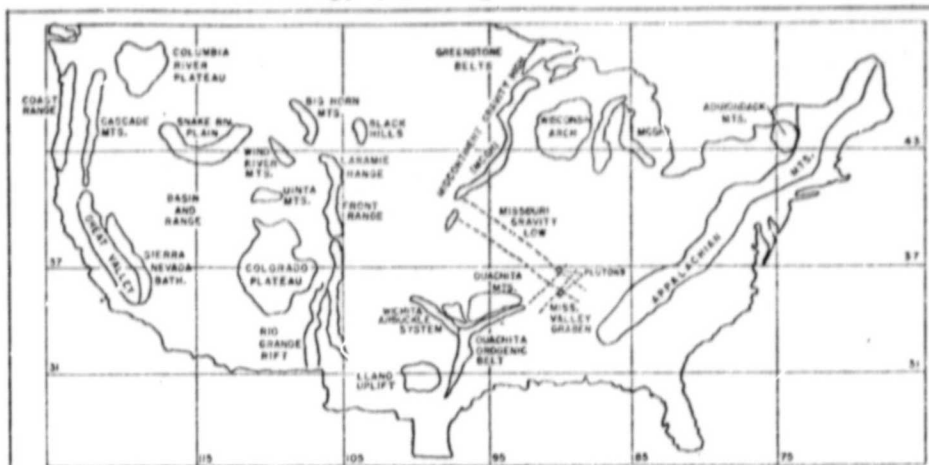

Fig. 5. Sketch map showing some of the major structures seen in the gravity anomaly maps presented in this paper. The Missouri gravity low can be seen best on the shaded relief map versions of the anomalies. The two plutons are the Bloomfield pluton to the north and the Covington pluton to the south. They can be seen as red dots on the Free air color maps and as bumps in the shaded relief anomaly maps. The Bloomfield intrusion is located at about 37°N, 90°W. The Mississippi valley graben location is from Kane et al. [1981], although the outline can be seen in the shaded relief anomaly maps.
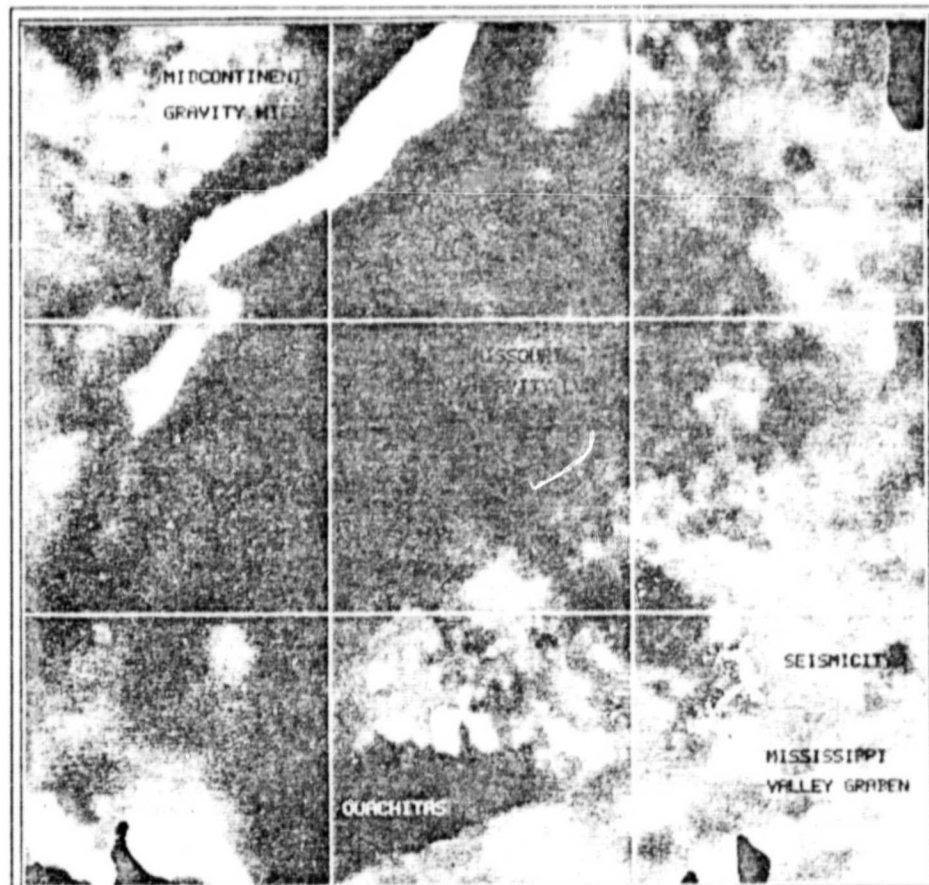

Fig. 6. Gray tone version of the filtered Free air anomalies. The map boundaries extend from 34° to 43°N, 87° to 99°W. The two horizontal lines correspond to 37° and 40°N latitude, while the two vertical lines are 91° and 95°W longitude. In this map, bright areas have large Free air anomalies, while dark areas have small (i.e., highly negative) values. The white dots are earthquake epicenters for the period from 1974–1979, as recorded by the St. Louis University seismic network. The Bloomfield and Covington plutons are the bright circular features just to the north and south, respectively, of the epicenter cluster. The Missouri gravity low extends from a break in the midcontinent gravity high, through Missouri, and across the Mississippi valley graben. The intersections of the gravity low and the graben are the locations of the intrusions. In addition, most of the seismicity is concentrated within the crustal block defined by the intersection of the gravity low and the graben.

and province boundaries defined by *Bickford et al.* [1981] in Missouri. For instance, the feature could have formed during the postulated collision event that produced the Grenville orogeny [*Dewey and Burke*, 1973].

Implications for the Earth Sciences

The future will see an increased availability of a number of other large, geographically oriented data sets that are applicable to earth science problems. For instance, as part of the National Uranium Resource Evaluation Program, the Department of Energy has acquired airborne digital gamma ray (net radioactivity) data, aeromagnetic anomalies, and hydrogeochemical data for most of the continental United States. Such large data sets are aptly suited for use with the kinds of techniques described in this paper. Of course, analysis of any data set requires, above all, the proper framing of scientific questions. Also, the right kinds of data must be accessible to answer the questions. However, we do feel that interactive digital image processing of a variety of geographically oriented data sets can lead to substantial advances in our understanding of the earth.

References

Batson, R. M., K. Edwards, E. M. Eliason, Computer-generated shaded relief images, *J. Res. U.S. Geol. Surv.*, 3, 401–408, 1975.

Blickford, M. E., K. Harrower, W. Hoppe, B. Nelson, R. Nusbaum, J. Thomas, Rb-Sr and U-Pb geochronology and distribution of rock types in the Precambrian basement of Missouri and Kansas, *Geol. Soc. Am. Bull.*, 92, 323–341, 1981.

Dewey, J. F., and K. Burke, Tibetan, Variscan, and Precambrian basement reactivation: Products of continental collision, *J. Geol.*, 81, 683–692, 1973.
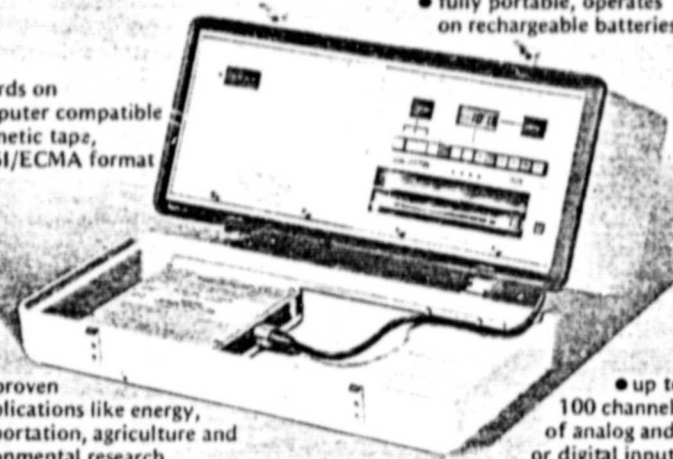
Eliason, E., and L. A. Soderblom, An array processing system for lunar geochemical and geophysical data, *Proc. Lunar Planet. Sci. Conf. 8th*, 1163–1170, 1977.

Ervin, C. P., and L. D. McGinnis, Reelfoot rift: Reactivited precursor to the Mississippi embayment, *Geol. Soc. Am. Bull.*, 86, 1287–1295, 1975.

Guinness, E. A., J. Strebeck, R. Arvidson, K. Schulz, G. Davies, Basement structure of the Ozark Plateau, Missouri-topography, gravity, seismic, and remote sensing data, submitted to *J. Geophys. Res.*, 1982.

Hildenbrand, T. G., M. F. Kane, and W. J. Stauder, Jr., Magnetic and gravity anomalies in the northern Mississippi embayment and their spacial relation to seismicity, *Misc. Field Stud. Map MF-914*, 2 sheets, U.S.

Geol. Surv., Reston, Va., 1977.

Kane, M. F., T. G. Hildenbrand, and J. D. Hendricks, Model for the tectonic evolution of the Mississippi embayment and its contemporary seismicity, *Geology*, 9, 563–568, 1981.

McGinnis, L. D., M. G. Wolf, J. J. Kohsmann, C. P. Ervin, Regional Free air anomalies and tectonic observations in the United States, *J. Geophys. Res.*, 84, 591–601, 1979.

McNutt, M., Implications of regional gravity for state of stress in the earth's crust and upper mantle, *J. Geophys. Res.*, 85, 6377–6396, 1981.

Moik, J. G., Digital processing of remotely sensed images, *Rep. SP-431*, 330 pp., Nat. Aeronaut. Space Admin., Washington, D.C., 1980.

Molnar, P., and P. Tapponnier, Cenozoic tectonics of Asia: Effects of a continental collision, *Science*, 189, 419–426, 1975.

Pettengill, G., E. Eliason, P. Ford, G. Loriot,

H. Masursky, Pioneer-Venus radar results: Altimetry and surface processes, *J. Geophys. Res.*, 85, 8261–8270, 1980.

Slater, P. N., Photographic systems for remote sensing, in *Manual of Remote Sensing*, edited by R. G. Reeves, pp. 235–323, American Society of Photogrammetry, Falls Church, Va., 1975.

Stauder, W., M. Kramer, G. Fischer, S. Schaeffer, and S. T. Morrissey, Seismic characteristics of southeast Missouri as indicated by a regional telemetered microearthquake array, *Bull. Seismol. Soc. Am.*, 66, 1953–1964, 1977.
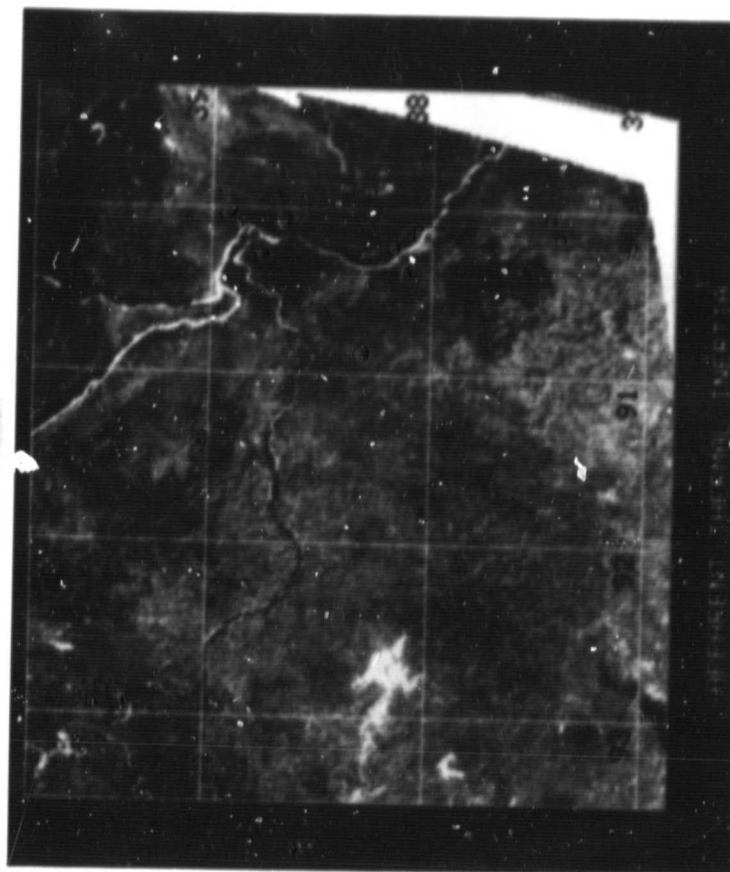
Strebeck, J. W., Structure of the Precambrian basement in the Ozark plateau as inferred from gravity and remote sensing data, Masters thesis, Washington University, St. Louis, Mo., 1982.

Woollard, G. P., and H. R. Joesting, Bouguer Gravity Anomaly Map of the United States, U.S. Geol. Surv., Reston, Va., 1964.

ORIGINAL PAGE IS
OF POOR QUALITY
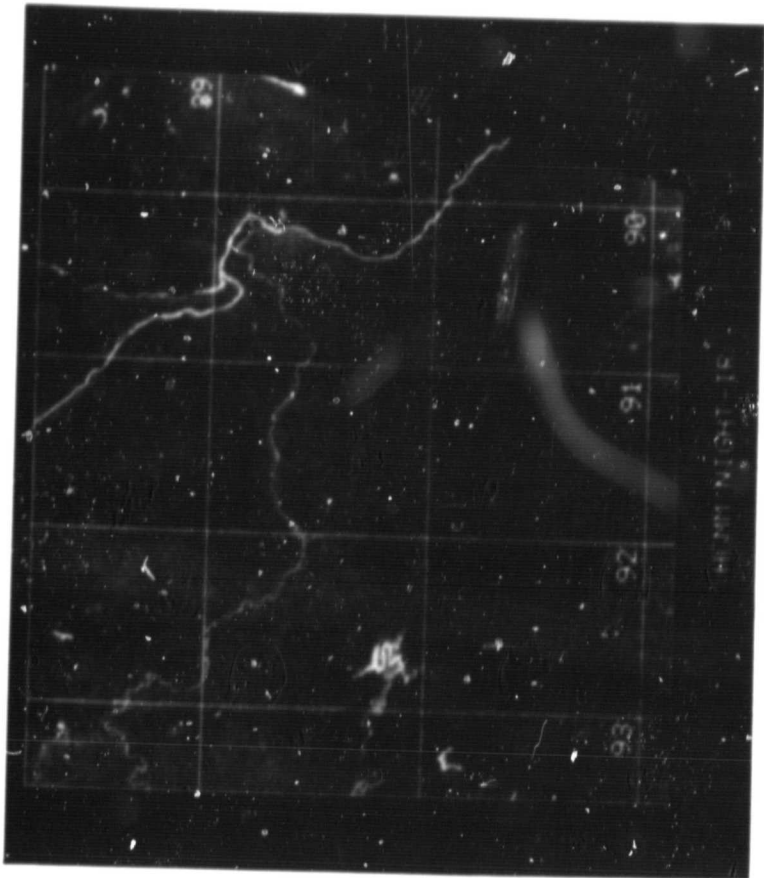
ORIGINAL PAGE
BLACK AND WHITE PHOTOGRAPH

ORIGINAL PAGE
BLACK AND WHITE PHOTOGRAPH